PMLevyCOLPEm Resource

From: Waters, David [David.Waters@pgnmail.com]
Sent: Monday, July 02, 2012 3:56 PM
To: Habib, Donald
Subject: NRC Letter 108 Draft Response - Pages 1-44
Attachments: NRC Letter 108 RAI L-0998 Response - Draft 07-02-12_Part1.pdf

First of three parts

Hearing Identifier: Levy_County_COL_Public
Email Number: 1156

Mail Envelope Properties (7FD614EFA33B03448166AF44364F42AE0E6786C097)

Subject: NRC Letter 108 Draft Response - Pages 1-44
Sent Date: 7/2/2012 3:55:30 PM
Received Date: 7/2/2012 3:55:39 PM
From: Waters, David

Created By: David.Waters@pgnmail.com

Recipients:
"Habib, Donald" <Donald.Habib@nrc.gov>
Tracking Status: None

Post Office: WN000075.oak.zone1.progress-energy.com

Files	**Size**	**Date & Time**	
MESSAGE	20	7/2/2012 3:55:39 PM	
NRC Letter 108 RAI L-0998 Response - Draft 07-02-12_Part1.pdf			806346

Options
Priority: Standard
Return Notification: No
Reply Requested: No
Sensitivity: Normal
Expiration Date:
Recipients Received:

NRC Letter 108 RAI (Seismic Hazards) Dated March 15, 2012

Evaluate the seismic hazard at your site against current NRC requirements and guidance and, if necessary, update the design basis and structures systems and components important to safety to protect against updated hazards (seismic portion only – of detailed Recommendation 2.1 – Enclosure 7 of SECY-12-0025).

Progress Energy Response L-0998 to NRC RAI:

Deleted: Outline

Sensitivity evaluations were performed to develop LNP site hard rock seismic hazard, finished grade 10^{-5} Uniform Hazard Response Spectra (UHRS), Ground Motion Response Spectra (GMRS), finished grade Performance Based Surface Response Spectra (PBSRS), and Foundation Interface Response Spectra (FIRS) (EL +11 ft.) using the Central and Eastern United States Seismic Source Characterization (CEUS SSC) (NUREG 2115) methodology and the modified cumulative absolute velocity (CAV) filter (NRC SECY-2012-0025 Enclosure 7 – Attachment 1 to Enclosure 1). The LNP site hard rock seismic hazard, finished grade 10^{-5} UHRS, GMRS, finished grade PBSRS, and FIRS (EL +11 ft.) using the CEUS SSC model were compared to the corresponding hazard and response spectra using the updated Electric Power Research Institute Seismic Owners Group (EPRI SOG) methodology. The updated EPRI SOG methodology included the updated EPRI SOG earthquake catalog through end of 2006 and use of the Updated Charleston Seismic Source (UCSS). It was concluded that the site specific designs (liquefaction evaluations, Soil Structure Interaction (SSI) analysis, and the evaluations for seismic interaction between the Annex Building (AB), Turbine Building (TB), and Radwaste Building (RB) with the nuclear island) for the CEUS SSC methodology ground motions are bounded by that for the updated EPRI SOG methodology currently presented in the FSAR. Similarly, the Seismic Margin Assessments for the standard plant components, site liquefaction potential, adjacent buildings' seismic interaction with the nuclear island, and the RCC bridging mat capacity for the CEUS SSC methodology ground motions are bounded by that for the updated EPRI SOG methodology currently presented in the FSAR.

Deleted: EPRI SOG

Deleted: EPRI SOG

Sensitivity Evaluations for CEUS SSC

Deleted: Evaluations

The CEUS SSC methodology, verification of the CEUS SSC methodology implementation, the LNP site hard rock seismic hazard, finished grade 10^{-5} UHRS, GMRS, finished grade PBSRS, FIRS (EL +11 ft.), and their comparison to the corresponding LNP site seismic hazards and amplified ground motions (to meet 10 CFR Part 50 Appendix S requirements) using the updated EPRI SOG model currently presented in the FSAR are presented in the new FSAR Subsection 2.5.2.7 included in this RAI response.

Deleted: EPRI SOG

Comparisons between the scaled GMRS, PBSRS, and FIRS developed using the updated EPRI-SOG model with full CAV and the corresponding spectra developed using the CEUS SSC model with modified CAV are shown on Figures 2.5.2-355, 2.5.2-357, and 2.5.2-358 respectively. These comparisons show that the PBSRS and FIRS based on the CEUS SSC model with modified CAV are enveloped by the corresponding spectra developed using the updated EPRI-SOG model with full CAV. The GMRS based on the CEUS SSC model with modified CAV is also nearly enveloped by the scaled GMRS based on the updated EPRI-SOG model with full CAV, with the maximum exceedance being 4 percent near 1 Hz. Thus, it is concluded that the site specific

ground motions developed using the updated EPRI-SOG model with full CAV presented in Subsection 2.5.2.6 are appropriate for use as the design basis for the LNP site.

The topics presented in the new FSAR Subsection 2.5.2.7 are as follows:

2.5.2.7 Sensitivity Evaluations for CEUS SSC
2.5.2.7.1 Summary of the CEUS SSC Model
2.5.2.7.2 Calculations for the Seven Demonstration Sites
2.5.2.7.2.1 Results for the Central Illinois Site
2.5.2.7.2.2 Results for the Chattanooga Site
2.5.2.7.2.3 Results for the Houston Site
2.5.2.7.2.4 Results for the Jackson Site
2.5.2.7.2.5 Results for the Manchester Site
2.5.2.7.2.6 Results for the Savannah Site
2.5.2.7.2.7 Results for the Topeka Site
2.5.2.7.2.8 Summary if Results of Calculations for the Demonstration Sites
2.5.2.7.3 Calculation of Hard Rock Hazard at the LNP Site Using the CEUS SSC Model
2.5.2.7.3.1 Implementation of the CEUS SSC Model for the LNP Site
2.5.2.7.3.2 Hard Rock Hazard Results for the LNP Site
2.5.2.7.3.3 Deaggregation of Hard Rock Hazard Results Based on the CEUS SSC Model
2.5.2.7.4 Calculation of GMRS, PBSRS, and FIRS at the LNP Site Using the CEUS SSC Model with Modified CAV
2.5.2.7.4.1 Inputs to the Calculation of the GMRS and PBSRS Using the the CEUS SSC Model and Modified CAV
2.5.2.7.4.2 Seismic Hazard Results for the CEUS SSC Model and Modified CAV
2.5.2.7.4.3 GMRS based on CEUS SSC Model and Modified CAV
2.5.2.7.4.4 PBSRS and FIRS based on CEUS SSC Model and Modified CAV
2.5.2.7.5 Summary of the Results of Sensitivity Analyses Using the CEUS SSC Model

Formatted: Bullets and Numbering

Deleted: ¶
¶

Scaled GMRS

For site specific evaluations and design (liquefaction evaluations, seismic interaction of the AB, TB, and RB with the NI, Soil Structure Interaction analysis of the NI, and the design of the RCC bridging mat), scaled PBSRS and scaled FIRS (EL +11 ft.) are used. The scale factor of 1/0.825 was used so that the FIRS has a zero period acceleration of 0.1g as required by 10 CFR Part 50 Appendix S. To be consistent with the site specific evaluations and design, the GMRS was also scaled by the 1/0.825 factor. The scaled horizontal and vertical GMRS are presented in Figure 2.5.2-296. The scaled GMRS represents the licensing basis GMRS for the LNP site.

The scaled horizontal and vertical GMRS are compared to the Westinghouse Certified Seismic Design Response Spectra (CSDRS) on Figure 2.5.2-296. The site scaled GMRS are enveloped by the CSDRS.

Site Liquefaction Evaluations

The soils under the nuclear island (NI) will be excavated and backfilled with Roller Compacted Concrete (RCC). Thus, no liquefaction potential exists under the NI

foundation. To evaluate the liquefaction potential of soils under the adjacent AB, TB, and RB, earthquake induced cyclic stresses in the soil column were based on ground motions consistent with the finished grade scaled PBSRS. As shown in Figure 2.5.2-357, the CEUS SSC PBSRS is enveloped by the updated EPRI SOG scaled PBSRS. Thus, the liquefaction evaluations based on the updated EPRI SOG LNP ground motions bound those from the CEUS SSC ground motions.

Deleted: RAI L-0998-3
Deleted: EPRI SOG
Deleted: EPRI SOG

Soil Structure Interaction Analysis

The scaled updated EPRI SOG scaled FIRS (EL +11 ft.) was the input ground motion for the LNP site specific SSI analysis. As shown in Figure 2.5.2-358 the horizontal and vertical CEUS SSC FIRS (EL +11 ft.) is enveloped by the corresponding updated EPRI SOG scaled FIRS (EL +11 ft.). Thus, the conclusions of the LNP site specific SSI analysis that the LNP floor response spectra (FRS) at the six key locations are bounded by the CSDRS FRS and the maximum bearing pressure is less than the 24 ksf design value are also valid for the for the LNP site ground motions based on the CEUS SSC model.

Deleted: EPRI SOG
Deleted: RA
Deleted: I L-0998-5
Deleted: , the
Deleted: EPRI SOG

Seismic Interaction between the Adjacent Buildings with the Nuclear Island

The updated EPRI SOG scaled finished grade PBSRS was used to show that there is no interaction between the adjacent AB, TB, and RB with the NI. As shown in Figure 2.5.2-357, the CEUS SSC finished grade horizontal and vertical PBSRS are enveloped by the updated EPRI SOG scaled finished grade PBSRS. Thus, the conclusions that there is no interaction between the adjacent AB, TB, and RB with the NI is valid for the LNP site ground motions based on the CEUS SSC model.

Deleted: EPRI SOG
Deleted: RAI L-0998-3
Deleted: is
Deleted: EPRI SOG

Seismic Margin Analysis

Deleted: margin

As shown in Figures 2.5.2-355 and 2.5.2-357, both the CEUS SSC GMRS and the PBSRS are enveloped by the AP1000 CSDRS. As stated above, the CEUS SSC LNP site specific floor response spectra (FRS) at the six key locations are bounded by the CSDRS FRS and the maximum bearing pressure is less than the 24 ksf design value. Thus, LNP site unique foundation conditions and CEUS SSC ground motions do not lower the High Confidence Low Probability of Failure (HCLPF) values calculated for the certified design.

Deleted: RAI L-0998-2
Deleted: RAI L-0998-3
Deleted: discussed

To evaluate the HCLPF liquefaction potential of soils under the adjacent AB, TB, and RB, earthquake induced cyclic stresses in the soil column based on ground motions consistent with the updated EPRI SOG finished grade 10^{-5} UHRS were used. As shown in Figures 3.7-228 and 3.7-229, 1.67*GMRS and 1.67*PBSRS developed using the CEUS SSC methodology and modified CAV filter are enveloped by the updated EPRI SOG finished grade 10^{-5} UHRS. Thus, HCLPF capacity for no liquefaction potential of soil under the AB, TB, and RB exceeds the 1.67*GMRS goal for the plant level HCLPF for the CEUS SSC ground motions.

Deleted: EPRI SOG
Deleted: RAI L-0998-6 and RAI L-0998-7
Deleted: EPRI SOG

To calculate the HCLPF capacity for seismic interaction between the AB, TB, and RB and the NI, the AB, TB, and RB displacements relative to the NI were calculated using the updated EPRI SOG finished grade 10^{-5} UHRS. As shown in Figures 3.7-228 and 3.7-229, 1.67*GMRS and 1.67*PBSRS developed using the CEUS SSC methodology and modified CAV filter are enveloped by the updated EPRI SOG finished grade 10^{-5} UHRS.

Deleted: EPRI SOG
Deleted: RAI L-0998-6 and RAI L-0998-7
Deleted: EPRI SOG

Thus, HCLPF capacity for no seismic interaction between the AB, TB, and RB and the NI exceeds the 1.67*GMRS goal for the plant level HCLPF for the CEUS SSC ground motions.

The HCLPF capacity of the RCC mat was calculated as 0.30g using the conservative deterministic failure margin (CDFM) methodology of FSAR Reference 19.55.7-201. The peak ground acceleration for the CEUS SSC GMRS is 0.073. Thus, the HCLPF capacity of the RCC bridging mat exceeds the overall plant HCLPF acceptance criteria of 1.67*GMRS using the CEUS SSC methodology and modified CAV filter.

Deleted: 1

Deleted: 0.30g

FSAR Text Revisions

Deleted: ¶

FSAR text revision are shown in the attached markup for Subsections 2.5.0, 2.5.2, 3.7, and 19.55

FSAR Chapter 2 Revised Tables

Deleted: ¶
¶

- Revised Table 2.0-201: Comparison of AP1000 DCD Site Parameters and LNP Site Characteristics
- Revised Table 2.5.2 226: LNP Site GMRS Scaled by 1.2121 consistent with Reactor Foundation Elevation SCOR FIRS Scaled to 0.1g Horizontal Peak Ground Acceleration

FSAR Chapter 2 New Tables

- Table 2.5.2-232: Comparison of Ground Motions Computed from Mean Hazard Curves for the Seven Demonstration Sites
- Table 2.5.2-233: Comparison of Reference and Deaggregation Earthquakes Based on Updated EPRI-SOG and CEUS SSC Models
- Table 2.5.2-234: Comparison of Updated EPRI SOG Scaled GMRS with CAV and CEUS GMRS with Modified CAV
- Table 2.5.2-235: Comparison of Updated EPRI SOG Scaled PBSRS with CAV and CEUS PBSRS with Modified CAV

FSAR Chapter 2 Revised Figures

- Revised Figure 2.5.2-294: Horizontal 10-5 UHRS, GMRS, and Scaled GMRS Based on CAV for the LNP Site.
- Revised Figure 2.5.2-296: Horizontal and Vertical Scaled GMRS for the LNP Site

FSAR Chapter 2 New Figures

- Figure 2.5.2-312: CEUS SSC model master logic tree
- Figure 2.5.2-313: Location of RLME sources in the CEUS SSC model. Approximate location of the LNP site is shown by the red star
- Figure 2.5.2-314: CEUS SSC model logic tree for the Mmax source zones
- Figure 2.5.2-315: Mmax source zones from the CEUS SSC model for the “narrow” interpretation. Approximate location of the LNP site is shown by the red star
- Figure 2.5.2-316: Mmax source zones from the CEUS SSC model for the

"wide" interpretation. Approximate location of the LNP site is shown by the red star

- Figure 2.5.2-317: CEUS SSC model logic tree for Seismotectonic source zones
- Figure 2.5.2-318: Map of Seismotectonic source zones for the "narrow" interpretation of PEZ and the Rough Creek Graben not included as part of the Reelfoot Rift (RR) source. Approximate location of the LNP site is shown by the red star
- Figure 2.5.2-319: Map of Seismotectonic source zones for the "narrow" interpretation of PEZ and the Rough Creek Graben included as part of the Reelfoot Rift (RR-RCG) source. Approximate location of the LNP site is shown by the red star
- Figure 2.5.2-320: Map of Seismotectonic source zones for the "wide" interpretation of PEZ and the Rough Creek Graben not included as part of the Reelfoot Rift (RR) source. Approximate location of the LNP site is shown by the red star
- Figure 2.5.2-321: Map of Seismotectonic source zones for the "wide" interpretation of PEZ and the Rough Creek Graben included as part of the Reelfoot Rift (RR-RCG) source. Approximate location of the LNP site is shown by the red star
- Figure 2.5.2-322: CEUS SSC model logic tree for the Charleston RLME source
- Figure 2.5.2-323: Alternative Charleston source geometries for the Charleston source
- Figure 2.5.2-324: Location of seven demonstration sites used for hazard calculations in NUREG-2115 and the location of the LNP site. Approximate location of the LNP site is shown by the red star
- Figure 2.5.2-325: Comparison of hazard curves computed using AMEC E&I software with those listed in Chapter 8 of NUREG-2115 for the Central Illinois demonstration site
- Figure 2.5.2-326: Comparison of hazard curves computed using AMEC E&I software with those listed in Chapter 8 of NUREG-2115 for the Chattanooga demonstration site
- Figure 2.5.2-327: Comparison of hazard curves computed using AMEC E&I software with those listed in Chapter 8 of NUREG-2115 for the Houston demonstration site
- Figure 2.5.2-328: Comparison of hazard curves computed using AMEC E&I software with those listed in Chapter 8 of NUREG-2115 for the Jackson demonstration site
- Figure 2.5.2-329: Comparison of hazard curves computed using AMEC E&I software with those listed in Chapter 8 of NUREG-2115 for the Manchester demonstration site
- Figure 2.5.2-330: Comparison of hazard curves computed using AMEC E&I software with those listed in Chapter 8 of NUREG-2115 for the Savannah

demonstration site

- Figure 2.5.2-331: Comparison of hazard curves computed using AMEC E&I software with those listed in Chapter 8 of NUREG-2115 for the Topeka demonstration site
- Figure 2.5.2-332: Comparison of hard rock hazard for 0.5 Hz spectral accelerations for the LNP Site computed using updated EPRI-SOG model with those obtained using the CEUS SSC model
- Figure 2.5.2-333: Comparison of hard rock hazard for 1 Hz spectral accelerations for the LNP Site computed using updated EPRI-SOG model with those obtained using the CEUS SSC model
- Figure 2.5.2-334: Comparison of hard rock hazard for 2.5 Hz spectral accelerations for the LNP Site computed using updated EPRI-SOG model with those obtained using the CEUS SSC model
- Figure 2.5.2-335: Comparison of hard rock hazard for 5 Hz spectral accelerations for the LNP Site computed using updated EPRI-SOG model with those obtained using the CEUS SSC model
- Figure 2.5.2-336: Comparison of hard rock hazard for 10 Hz spectral accelerations for the LNP Site computed using updated EPRI-SOG model with those obtained using the CEUS SSC model
- Figure 2.5.2-337: Comparison of hard rock hazard for 25 Hz spectral accelerations for the LNP Site computed using updated EPRI-SOG model with those obtained using the CEUS SSC model
- Figure 2.5.2-338: Comparison of hard rock hazard for 100 Hz spectral accelerations (PGA) for the LNP Site computed using updated EPRI-SOG model with those obtained using the CEUS SSC model
- Figure 2.5.2-339: Contribution of the various source types to the total mean hazard at the LNP Site
- Figure 2.5.2-340: Comparison of hard rock UHRS based on updated EPRI-SOG model with results computed using the CEUS SSC model
- Figure 2.5.2-341: Deaggregation of mean 10-3 hazard from CEUS SSC model calculations
- Figure 2.5.2-342: Deaggregation of mean 10-4 hazard from CEUS SSC model calculations
- Figure 2.5.2-343: Deaggregation of mean 10-5 hazard from CEUS SSC model calculations
- Figure 2.5.2-344: Deaggregation of mean 10-6 hazard from CEUS SSC model calculations
- Figure 2.5.2-345: Comparison of mean hazard curves for 0.5 Hz spectral acceleration computed with CAV for the finished grade elevation (left) and the GMRS elevation (right). Solid lines are results for the updated EPRI-SOG model with CAV applied to all magnitudes and dashed lines are for the CEUS SSC model with CAV applies only to magnitudes < M 5.5
- Figure 2.5.2-346: Comparison of mean hazard curves for 1 Hz spectral

acceleration computed with CAV for the finished grade elevation (left) and the GMRS elevation (right). Solid lines are results for the updated EPRI-SOG model with CAV applied to all magnitudes and dashed lines are for the CEUS SSC model with CAV applies only to magnitudes < M 5.5

- Figure 2.5.2-347: Comparison of mean hazard curves for 2.5 Hz spectral acceleration computed with CAV for the finished grade elevation (left) and the GMRS elevation (right). Solid lines are results for the updated EPRI-SOG model with CAV applied to all magnitudes and dashed lines are for the CEUS SSC model with CAV applies only to magnitudes < M 5.5
- Figure 2.5.2-348: Comparison of mean hazard curves for 5 Hz spectral acceleration computed with CAV for the finished grade elevation (left) and the GMRS elevation (right). Solid lines are results for the updated EPRI-SOG model with CAV applied to all magnitudes and dashed lines are for the CEUS SSC model with CAV applies only to magnitudes < M 5.5
- Figure 2.5.2-349: Comparison of mean hazard curves for 10 Hz spectral acceleration computed with CAV for the finished grade elevation (left) and the GMRS elevation (right). Solid lines are results for the updated EPRI-SOG model with CAV applied to all magnitudes and dashed lines are for the CEUS SSC model with CAV applies only to magnitudes < M 5.5
- Figure 2.5.2-350: Comparison of mean hazard curves for 25 Hz spectral acceleration computed with CAV for the finished grade elevation (left) and the GMRS elevation (right). Solid lines are results for the updated EPRI-SOG model with CAV applied to all magnitudes and dashed lines are for the CEUS SSC model with CAV applies only to magnitudes < M 5.5
- Figure 2.5.2-351: Comparison of mean hazard curves for 100 Hz spectral acceleration computed with CAV for the finished grade elevation (left) and the GMRS elevation (right). Solid lines are results for the updated EPRI-SOG model with CAV applied to all magnitudes and dashed lines are for the CEUS SSC model with CAV applies only to magnitudes < M 5.5
- Figure 2.5.2-352: Comparison of UHRS for the GMRS elevation based on updated EPRI-SOG model with full CAV and the CEUS SSC model with modified CAV.
- Figure 2.5.2-353: Comparison of UHRS for the PBSRS elevation based on the updated
- EPRI-SOG model with full CAV and the CEUS SSC model with modified CAV
- Figure 2.5.2-354: Development of horizontal GMRS based on the CEUS SSC model with modified CAV
- Figure 2.5.2-355: Comparison of GMRS based on updated EPRI-SOG and CEUS SSC models
- Figure 2.5.2-356: Development of horizontal PBSRS based on the CEUS SSC model with modified CAV
- Figure 2.5.2-357: Comparison of PBSRS based on updated EPRI-SOG and CEUS SSC models
- Figure 2.5.2-358: Comparison of Reactor Building FIRS based on updated EPRI-SOG and CEUS SSC models

FSAR Chapter 3 New Figures

- Figure 3.7-228: Comparison of 1.67*GMRS developed using the CEUS SSC methodology and modified CAV filter with the updated EPRI SOG 10^{-5} UHRS
- Figure 3.7-229: Comparison of 1.67* PBSRS, developed using the CEUS SSC methodology and modified CAV filter, with the updated EPRI SOG 10-5

FSAR Chapter 19 Revised Table

- Revised Table 19.55-201: HCLPF Capacities for LNP Site Specific Design Features

Deleted: ¶

Formatted: Bullets and Numbering

Formatted: Bullets and Numbering

Deleted: ¶
¶

Levy Nuclear Plant Units 1 and 2
COL Application
Part 2, Final Safety Analysis Report

LNP SUP 2.0-1

Table 2.0-201 (Sheet 2 of 9)
Comparison of AP1000 DCD Site Parameters and LNP Site Characteristics

	AP 1000 DCD Site Parameters	LNP Site Characteristics	LNP Site Characteristic Reference	Bounding Yes/No
Seismic				
CSDRS	CSDRS free field peak ground acceleration of 0.30 g with modified Regulatory Guide 1.60 response spectra (see Figures 5.0-1 and 5.0-2.). The SSE is now referred to as CSDRS. Seismic input is defined at finished grade except for sites where the nuclear island is founded on hard rock. If the site-specific spectra exceed the response spectra in Figures 5.0-1 and 5.0-2 at any frequency, or if soil conditions are outside the range evaluated for AP1000 design certification, a site-specific evaluation can be performed. This evaluation will consist of a site-specific dynamic analysis and generation of in-structure response spectra at key locations to be compared with the floor response spectra of the certified design at 5 percent damping. The site is acceptable if the floor response spectra from the site-specific evaluation do not exceed the AP1000 spectra for each of the locations or the exceedances are justified. The HRHF envelope response spectra are shown in Figure 5.0-3 and Figure 5.0-4 defined at the foundation level for 5 percent damping. The HRHF envelope response spectra provide an alternative set of spectra for evaluation of site-specific GMRS. A site is acceptable if its site-specific GMRS falls within the AP1000 HRHF envelope response spectra. Evaluation of a site for application of the HRHF envelope response spectra includes consideration of the limitation on shear wave velocity identified for use of the HRHF envelope response spectra. This limitation is defined by a shear wave velocity at the bottom of the basemat equal to or higher than 7,500 ft/sec, while maintaining a shear wave velocity equal to or above 8,000 ft/sec at the lower depths. (d)	For updated EPRI SOG scaled GMRS peak ground accelerations: 0.084 g horizontal 0.062 g vertical For CEUS SSC GMRS peak ground accelerations: 0.073 g horizontal 0.054 g vertical GMRS peak ground acceleration defined at 100 Hz. Ground Response Spectra: At LNP 1 and LNP 2: The horizontal and vertical updated EPRI SOG scaled GMRS and CEUS SSC GMRS are bounded by the horizontal and vertical CSDRS (Figure 2.5.2-355)	FSAR Subsections 2.5.2.6, 2.5.2.7 and 3.7	Yes

Deleted: 069
Deleted: 051
Deleted: 2.5.2-296
Deleted: .

separating the Upper Floridan aquifer within the Avon Park Formation from the Lower Floridan aquifer within the Oldsmar Limestone.

The LNP site stratigraphy and surface morphology are consistent with expected characteristics of a developed, older (paleo) karst landscape mantled by several meters of sand (i.e., a mantled epikarst subsurface). Although there are no recognized sinkholes in the State of Florida sinkhole database or the SDII Global Corporation's much larger, private database (Reference 2.5.1-328) within 2 km (1.28 mi.) of the LNP site and no sinkholes at the land surface were observed during site investigations and reconnaissance within the LNP site, the presence of a few voids at depths identified in some borings suggests that paleo sinks such as those developed on the barren mature epikarst surface are locally present at the site.

Based on the review and updating of the geological, seismological, geophysical, and geotechnical data for the LNP site, nothing was identified that would preclude the safe operation of the facilities. The only geologic hazard identified in the LNP site area is potential surface deformation related to carbonate dissolution and slow cover subsidence related to the occurrence of karst. Karst features encountered below the nuclear islands at the LNP site are determined to be associated with near-vertical to vertical fractures and subhorizontal bedding planes, and vary in size from a few centimeters to approximately 1.5 m (5 ft.). Karst-related solution zones and/or infilled zones that exist in the subsurface beneath the LNP foundation will be addressed through appropriate design considerations in the LNP foundation conceptual design, as described in FSAR Subsection 2.5.4.

2.5.0.2 Vibratory Ground Motion

The selected starting point for developing the site-specific ground motion assessments for the LNP site was the Probabilistic Seismic Hazard Analysis (PSHA) conducted by the EPRI-SOG in the 1980s. Following guidance in the U.S. Nuclear Regulatory Commission (NRC) Regulatory Guide 1.208, the adequacy of the EPRI-SOG hazard results was evaluated in light of new data and interpretations and evolving knowledge pertaining to seismic hazard evaluation in the central and eastern United States (CEUS). PSHA sensitivity analyses were conducted to test the effect of the new information on the seismic hazard. Using these results, a PSHA analysis was performed using an updated EPRI-SOG seismic source model. The results of that analysis are used to develop the site-specific design ground motions. The site specific ground motions were scaled upward to meet 10 CFR Part 50 Appendix S requirements.

Sensitivity evaluations were performed for using the the CEUS SSC seismic source model (NUREG-2115) and the modified CAV filter (SECY-2012-0025 Enclosure 7 – Attachment 1 to Enclosure 1) to show that the site specific ground response spectra obtained using the CEUS SSC are bounded by those using the updated EPRI SOG methodology scaled to meet 10 CFR Part 50 Appendix S requirements. The CEUS SSC sensitivity evaluations are described in Subsection 2.5.2.7.

Deleted: n updated

Deleted: ;

Deleted: t

Deleted: have been

Deleted: uniform hazard response spectra (UHRS) and the identification of the controlling earthquakes

Deleted: Reference 2.5.2-284

Deleted: 4

generated and the mean site amplification (response spectrum for surface motion divided by response spectrum for input motion) was computed.

Based on sensitivity analyses, two profiles (one for each unit) were selected for calculation of the site amplification. The envelope of the site amplification computed from the two profiles was used to develop surface motion.

The site response analyses profiles for the design grade case were developed by adding a layer of engineered fill to the GMRS profiles to bring the top elevation up to 15.5 m (51 ft.) NAVD88. The analyses were performed for a wide range of engineered fill properties.

2.5.0.2.6 Ground Motion Response Spectra

The final assessment of the surface UHRS was based on PSHA calculations that use cumulative absolute velocity (CAV) filtering in place of a fixed minimum magnitude. These UHRS were used to develop the GMRS.

The horizontal GMRS for the LNP site were developed using the performance-based approach defined in NRC Regulatory Guide 1.208 (based on UHRS developed using CAV filtering). The computed GMRS corresponds to the minimum of 0.45 times the 10^{-5} USRS. The vertical GMRS were developed by multiplying the horizontal GMRS by vertical/horizontal spectral ratios derived from the ratios recommended for western United States (WUS) rock and CEUS hard rock in NUREG/CR-6728. A final step was to scale the GMRS upward to mean the requirement of a minimum peak horizontal acceleration of 0.1 gravity acceleration (g) at the reactor foundation level. The horizontal and vertical site scaled GMRS are enveloped by the Westinghouse Certified Seismic Design Response Spectra (CSDRS).

Performance-based surface response spectra (PBSRS) and associated soil column outcropping response (SCOR) foundation input response spectra (FIRS) were developed using the site response analysis of profiles that extended to the design grade elevation. These spectra were scaled upward to meet the requirement of a minimum peak horizontal acceleration of 0.1 gravity acceleration (g) at the reactor foundation level. These spectra are used to develop inputs for soil structure interaction (SSI) analyses. The scaled PBSRS are also enveloped by the Westinghouse CSDRS. Design grade (elevation 15.5 m [51 ft.]) SSI input response spectra were also developed. Three SSI input soil profiles were developed from the randomized soil profiles used to compute the PBSRS. These profiles accommodate the variability in the in-situ materials and the anticipated range in fill properties.

2.5.0.3 Surface Faulting

2.5.2 VIBRATORY GROUND MOTION

LNP COL 2.5-2

This subsection provides a detailed description of vibratory ground motion assessments that were carried out for LNP 1 and LNP 2. The subsection begins with a review of the approaches outlined in NRC Regulatory Guide 1.208 for conducting the vibratory ground motion studies. Following this review of the regulatory framework used for the project, results of the seismic hazard evaluation are documented and the site-specific scaled GMRS for horizontal and vertical motions are developed. In addition, sensitivity evaluations were performed for the CEUS SSC source model (NUREG-2115) and the modified CAV filter (SECY-2012-0025 Enclosure 7 – Attachment 1 to Enclosure 1) to show that the site specific groung response spectra (PBSRS and FIRS (EL +11 ft.)) obtained using the CEUS SSC model are bounded by those obtained using the updated EPRI SOG model scaled to meet 10 CFR Part 50 Appendix S requirements. The updated EPRI SOG methodology included the updated EPRI SOG earthquake catalog through end of 2006 and use of the Updated Charleston Seismic Source (UCSS). The CEUS SSC sensitivity evaluations are described in Subsection 2.5.2.7.

Deleted: Reference 2.5.2-284

The NRC Regulatory Guide 1.208 provides guidance on methods acceptable to the NRC to satisfy the requirements of the seismic and geologic regulation, 10 Code of Federal Regulations (CFR) 100.23, for assessing the appropriate safe shutdown earthquake (SSE) ground motion levels for new nuclear power plants. Regulatory Guide 1.208 states that the PSHA conducted by the EPRI-SOG in the 1980s (References 2.5.2-201 and 2.5.2-202) has been used for studies in the past. The EPRI-SOG study involved a comprehensive compilation of geological, geophysical, and seismological data; evaluations of the scientific knowledge concerning earthquake sources, maximum earthquakes, and earthquake rates in the CEUS by six multidisciplinary teams of experts in geology, seismology, and geophysics; and separately, development of state-of-knowledge earthquake ground motion modeling, including epistemic and aleatory uncertainties.[c] The uncertainty in characterizing the frequency and maximum magnitude of potential future earthquakes associated with these sources and the ground motion that may be produced was assessed and explicitly incorporated in the seismic hazard model.

c. Epistemic uncertainty is uncertainty attributable to incomplete knowledge about a phenomenon that affects the ability to model it. Epistemic uncertainty is reflected in a range of viable models, model parameters, multiple expert interpretations, and statistical confidence. In principle, epistemic uncertainty can be reduced by the accumulation of additional information. Aleatory uncertainty (often called aleatory variability or randomness) is uncertainty inherent in a nondeterministic (stochastic, random) phenomenon. Aleatory uncertainty is accounted for by modeling the phenomenon in terms of a probability model. In principle, aleatory uncertainty cannot be reduced by the accumulation of more data or additional information.

Regulatory Guide 1.208 further specifies that the adequacy of the EPRI-SOG hazard results must be evaluated in light of new data and interpretations and evolving knowledge pertaining to seismic hazard evaluation in the CEUS. The following steps describe a procedure acceptable to the NRC staff for performing a PSHA.

1. Perform regional and site geological, seismological, and geophysical investigation in accordance with Regulatory Position 1 and Appendix C to RG 1.208.

2. Perform an evaluation of seismic sources, in accordance with Appendix C to RG 1.208, to determine whether they are consistent with the site-specific data gathered in Regulatory Positon 3.1 or if they require updating. If potentially significant differences are identified, perform sensitivity analyses to assess whether those differences have a significant effect on site hazard.

3. If Step 2 indicates that there are significant differences in site hazard, then the PSHA for the site is revised by either updating the previous calculations or, if necessary, performing a new PSHA. If not, the previous EPRI-SOG results may be used to assess the appropriate SSE ground motions.

Regulatory Guide 1.208 provides guidance on performance goal-based methods acceptable to the NRC to satisfy the requirements of the seismic and geologic regulation, 10 CFR 100.23, for assessing the appropriate site-specific performance goal-based ground motions for new nuclear power plants. Specifically, the performance-based approach described in American Society of Civil Engineers/Structural Engineering Institute (ASCE/SEI) Standard 43-05, "Seismic Design Criteria for Structures, Systems, and Components in Nuclear Facilities" may be used to define site-specific performance goal-based GMRS at the ground surface based on mean hazard results (Reference 2.5.2-203). The development of mean seismic hazard results is to be based on a site-specific PSHA combined with site-specific site amplification analyses. The procedures to be used to perform the PSHA and site amplification studies are in Regulatory Guide 1.208. Regulatory Guide 1.208 also provides guidance on an alternative approach for addressing the lower-bound magnitude used in the PSHA based on the likelihood that earthquakes of various sizes can produce potentially damaging ground motions. The ground motion measure used to correlate with the threshold of potential damage is cumulative absolute velocity (CAV). The alternative approach using the CAV filter is used to develop the final scaled GMRS for LNP 1 and 2.

This subsection discusses the following aspects of vibratory ground motion:

- Seismicity (FSAR Subsection 2.5.2.1)

- Geologic and Tectonic Characteristics of the Site and Region (FSAR Subsection 2.5.2.2)
- Correlation of Earthquake Activity with Seismic Sources (FSAR Subsection 2.5.2.3)
- Probabilistic Seismic Hazard Analysis and Controlling Earthquake (FSAR Subsection 2.5.2.4)
- Seismic Wave Transmission Characteristics of the Site (FSAR Subsection 2.5.2.5)
- Ground Motion Response Spectra (FSAR Subsection 2.5.2.6)
- Sensitivity Evaluations for the CEUS SSC model (FSAR Subsection 2.5.2.7)

2.5.2.1 Seismicity

An important component in developing a seismic hazard model for the LNP site is the seismic history of the region. The selected starting point for developing the site-specific PSHA for the LNP site is the EPRI-SOG (Reference 2.5.2-201) seismic hazard model for the CEUS. The data used to assess earthquake occurrence rates for the seismic sources in the EPRI-SOG model were those in the earthquake catalog.

The first step in the three-step process for evaluating the adequacy of this model for the assessment of seismic hazards at the LNP site involved an assessment of the effect of recent information on the characterization of the seismicity of the southeastern United States. The development of an updated earthquake catalog for the project region is described in FSAR Subsection 2.5.2.1.1. Information on significant earthquakes is provided in FSAR Subsection 2.5.2.1.2. In addition to the discussion of significant earthquakes within the site region, this subsection also discusses recent earthquakes in Gulf of Mexico that postdate the EPRI-SOG catalog. Although these events fall outside the 320-km (200-mi.) radius site region, they occurred within some of the EPRI-SOG background seismic source zones that include the LNP site and thus have implications for assessment of maximum magnitudes in these source zones as discussed in FSAR Subsection 2.5.2.4.1.2. In addition, further assessment of catalog completeness and earthquake recurrence parameters for the offshore region were required as discussed in FSAR Subsections 2.5.2.4.1.3 and 2.5.2.4.1.4.

2.5.2.1.1 Earthquake Catalog

Earthquake occurrence rates for the seismic sources developed in the EPRI-SOG study were based on the EPRI-SOG CEUS earthquake catalog that was developed for the time period of 1627 through February 1985. The EPRI-SOG catalog has gone through two significant revisions. Seeber and Armbruster (Reference 2.5.2-204) conducted a thorough review of the catalog,

Deleted: 4

combination of Source 24 active within the boundary of Source 103 produced slightly higher hazard than the other cases. This combination was used in the updated hazard analysis. The hazard curve for Source 103 shown on Figure 2.5.2-224 includes the contribution of Source 24.

2.5.2.4.3.1.6 Woodward-Clyde Consultants Team's Seismic Sources

Figure 2.5.2-224 shows the mean hazard curves computed for the Woodward-Clyde Consultants team's sources listed in Table 2.5.2-207. The Gulf Coast ground motion model was applies to Source B36. This source is the largest contributor to the hazard at the LNP site from the Woodward-Clyde Consultants source model.

The two alternative geometries for Source 31 were tested. It was found that they produced very similar hazard, with Alternative 31 producing slightly higher hazard than Alternative 31A. In order to simplify the model, only the Alternative 31 is shown on Figure 2.5.2-224 and this alternative was used in the updated seismic hazard analysis.

2.5.2.4.3.2 PSHA Sensitivity to Revisions of the EPRI-SOG Sources

FSAR Subsection 2.5.2.4.1.2 discusses modifications to the maximum magnitude distributions for EPRI-SOG seismic sources that extend into the Gulf of Mexico and encompass the location of one or both of the moderate magnitude earthquakes that occurred in 2006. The effect of these modified maximum magnitude distributions on the hazard from the EPRI-SOG seismic sources is shown on Figure 2.5.2-225. The modified maximum magnitude distributions primarily affect the source zones in which the LNP site is located and the result is an appreciable increase in the hazard.

FSAR Subsection 2.5.2.4.1.4 presents an updated assessment of catalog completeness and seismicity parameters for the region in the Gulf of Mexico that was not included in the original EPRI-SOG calculation of seismicity parameters. The affect of including the updated seismicity rates for these sources is also shown on Figure 2.5.2-225. The result is a small increase in the hazard from sources that extend into the Gulf of Mexico in the vicinity of the site.

In summary, the modifications to the maximum magnitude distributions to account for the occurrence of the 2006 Gulf of Mexico earthquakes and to incorporate Gulf of Mexico seismicity lead to a combined appreciable increase in the hazard at the LNP site from the updated EPRI-SOG seismic sources, and these modifications are incorporated into the updated PSHA for the LNP site. The limitation on the maximum magnitude distribution for EPRI-SOG Charleston-specific seismic sources is considered to be appropriate to prevent double counting of the occurrence of large-magnitude earthquakes near Charleston and is also incorporated into the updated PSHA for the LNP site.

2.5.2.4.4 PSHA for the LNP Site

The PSHA for the LNP site was conducted using the updated EPRI-SOG seismic sources described in FSAR Subsection 2.5.2.4.2.1 which included the UCSS source described in FSAR Subsection 2.5.2.4.2.2. Earthquake ground motions were modeled using the median ground motion models and the ground motion aleatory variability models developed by EPRI (References 2.5.2-253 and 2.5.2-258). The logic tree defining the epistemic uncertainty in the ground motion characterization is shown on Figure 2.5.2-217.

Deleted: combined with

The hazard analysis was conducted using the m_b magnitude scale because the earthquake occurrence rates for the EPRI-SOG seismic sources are defined in terms of m_b magnitudes. Epistemic uncertainty in the conversion from m_b magnitudes to moment magnitudes for ground motion estimation was modeled by using the three equally weighted conversion relationships listed on Figure 2.5.2-217. Conversion of the moment magnitude estimates for the size of the repeated earthquakes associated with the UCSS into m_b magnitudes for summation of the hazard was done in a consistent manner such that the original value of **M** was recovered for ground motion estimation. For example, when the Atkinson and Boore (Reference 2.5.2-255) relationship was used to convert m_b to **M** for ground motion estimation, its inverse was used to convert the **M** values for the UCSS earthquakes into m_b values.

Earthquakes occurring in the updated EPRI-SOG seismic sources were modeled as point sources, and the EPRI models for distance adjustment and additional aleatory variability resulting from the use of point sources (epicenter) to model earthquakes were applied (Reference 2.5.2-253). The models based on the assumption of a random rupture location with respect to the epicenter were used. Earthquakes occurring on the UCSS source of repeated large earthquakes and postulated ECFS sources were modeled as extended ruptures, and the distance adjustment and additional aleatory variability models were not applied to these sources.

EPRI concluded that there was no basis for truncation of the lognormal distribution for ground motion amplitude other than the strength of the subsurface materials (Reference 2.5.2-258). Accordingly, untruncated lognormal distributions for earthquake ground motions were used in the PSHA.

The EPRI ground motion models represent the ground motions for a generic hard rock condition in the CEUS (Reference 2.5.2-253). Thus the site-specific PSHA results presented in this subsection represent the motions on outcropping rock with a shear-wave velocity in excess of about 2743 m/sec (9000 ft/sec). The effect of the sediments overlying this generic rock condition on defining the hazard at other locations is addressed in FSAR Subsections 2.5.2.5 and 2.5.2.6.

The initial generic CEUS hard rock hazard was computed using a fixed lower-bound magnitude of m_b 5.0. These results were used to develop the appropriate response spectra and time histories for the site response analyses. Once the site amplification functions were developed, a second hazard

Deleted: 4

response over the range of engineered fill velocities produces different behavior when assessing the probabilistic surface response spectra.

2.5.2.6 Ground Motion Response Spectra

LNP COL 2.5-3 2.5.2.6.1 Surface Spectra

Surface hazard spectra for the LNP GMRS profiles are obtained by scaling the rock RE and UHRS by the site amplification functions. The process used is illustrated on Figure 2.5.2-285 for the 10^{-4} level ground motions.

- The reference (controlling) spectra for LF and HF motions developed for each annual exceedance level were scaled by the appropriate smoothed amplification function to produce ground surface spectra.
- The generic hard rock UHRS was also scaled using the appropriate LF and HF amplification values.
- A smooth envelope of the scaled spectra is constructed to define the surface 10^{-4} UHRS.

The rock UHRS exhibit a sharp peak at 25 Hz. This peak is an artifact of the fact that the PSHA is computed for frequencies of 10, 25, and 100 Hz and that the RE spectra are defined for frequencies in the range of 5 to 10 Hz. The spectral shapes for CEUS earthquakes developed in McGuire et al. (Reference 2.5.2-256) show a broader peak in the spectrum in the frequency range of 10 to 100 Hz. Therefore, the approach described in FSAR Subsection 2.5.2.4.4.3 was used to smoothly interpolate the rock UHRS between 10 and 100 Hz. An additional HF RE spectral shape was constructed to match the rock UHRS at 25 Hz. This shape was then adjusted to match the UHRS at 10 and 100 Hz by applying adjustment factors that varied linearly with log frequency from 0 at 25 Hz to the appropriate value at 10 or 100 Hz. This smoothed rock UHRS was then multiplied by the HF amplification function.

Similar operations were performed to develop GMRS profile surface spectra for the 10^{-5} and 10^{-6} exceedance level motions. This smooth envelope spectrum represents the surface UHRS for the site defined as free field surface motions for a soil column truncated at elevation 11 m (36 ft.) NAVD88, the top of the first competent layer.

The above process was followed to develop design grade surface response spectra at elevation 15.5 m (51 ft.) NAVD88. For this case a weighted combination of the amplification functions for the three engineered fill velocities was used to construct a single surface spectrum for each level of input ground motion. The range of engineered fill velocity provided in Table 2.5.4.5-201 was treated as representing the 90 percent confidence interval for the epistemic uncertainty on the average engineered fill velocity. The three-point distribution

Deleted: 4

Levy Nuclear Plant Units 1 and 2
COL Application
Part 2, Final Safety Analysis Report

2.5.2.6.3 Horizontal GMRS

Regulatory Guide 1.208 defines the GMRS as a risk-consistent design response spectrum computed from the site-specific UHRS at a mean annual frequency of exceedance of 10^{-4} by the relationship:

$$GMRS = DF \times UHRS\ (10^{-4}) \qquad \text{Equation 2.5.2-215}$$

Parameter *DF* is the design factor specified by the expression:

$$DF = \text{Maximum}\ (1.0,\ 0.6(A_R)^{0.8}) \qquad \text{Equation 2.5.2-216}$$

In which A_R is the ratio of the UHRS ground motions for annual exceedance frequencies of 10^{-4} and 10^{-5}, specifically:

$$A_R = \frac{UHRS(10^{-5})}{UHRS(10^{-4})} \qquad \text{Equation 2.5.2-217}$$

Regulatory Guide 1.208 also specifies that when the value of A_R exceeds 4.2, the amplitude of the GMRS is to be no less than 0.45 × $SA(0.1H_D)$ that is, 45 percent of the 10^{-5} UHRS. As the 10^{-4} UHRS with CAV is 0, this second criteria is used to define the horizontal GMRS. Figure 2.5.2-294 shows the horizontal GMRS calculated as 0.45 × $SA(0.1H_D)$.

For site specific evaluations and design (liquefaction evaluations, seismic interaction of the Auxillary Building, Turbine Building, and Radwaste Building with the Nuclear Island, Soil Structure Interaction analysis of the NI, and the design of the RCC bridging mat), scaled PBSRS and scaled FIRS described in Subsectionare 2.5.2.6.6 are used. The scale factor of 1/0.825 was used so that the FIRS has a zero period acceleration of 0.1g as required by 10 CFR Part 50 Appendix S. To be consistent with the site specific evaluations and design, the horizontal GMRS was also scaled by the 1/0.825 factor. The scaled horizontal GMRS is listed in Table 2.5.2-226 along with the 10^{-5} UHRS and is shown on Figure 2.5.2-294. The scaled horizontal GMRS represents the licensing basis horizontal GMRS for the LNP site.

Deleted: value

Deleted: These values are listed in Table 2.5.2-226 along with the horizontal mean 10^{-5} UHRS.¶

Deleted: 0

Deleted: 0

2.5.2.6.4 Vertical GMRS

The vertical GMRS were developed from the horizontal GMRS using vertical to horizontal (V/H) spectral ratios recommended by McGuire et al. (Reference 2.5.2-263). These are given as a function of frequency for three levels of horizontal peak acceleration. Given the low amplitude of the horizontal GMRS of the LNP site, both unscaled and scaled, the V/H ratios for peak acceleration less than 0.2g are used. These ratios are plotted on Figure 2.5.2-295 for the WUS and CEUS.

Deleted:

McGuire et al. (Reference 2.5.2-263) indicate that V/H for intermediate sites can be obtained as a weighted combination of the V/H for WUS rock and CEUS rock

Deleted: 4

with the weights determined as a function of the site κ relative to the CEUS κ of 0.006 seconds and the WUS κ of 0.04 seconds. However, computing a weighted combination would flatten the WUS and CEUS peaks in V/H at spectral frequencies of 17 and 63 Hz, respectively, without producing a peak at an intermediate frequency. It is likely that sites with intermediate values of κ would have peaks in the V/H ratios of comparable amplitude but at an intermediate frequency.

Accordingly, an intermediate V/H ratio was developed for the LNP site by first shifting the WUS and CEUS V/H amplitudes to an intermediate frequency and then averaging their amplitudes. The best estimate value of κ for the LNP site is intermediate between the WUS and CEUS values. The WUS and CEUS V/H shapes were thus shifted to a frequency midway in log space between the two. The resulting V/H ratio is shown on Figure 2.5.2-295. In computing the intermediate V/H, a minimum value of 0.5 was used for the WUS V/H ratios to make them consistent in shape to the CEUS V/H ratios. A vertical scaled GMRS was then computed by multiplying the horizontal scaled GMRS by this V/H ratio. The resulting vertical scaled GMRS is listed in Table 2.5.2-226 along with the values of V/H.

Deleted: ¶

2.5.2.6.5 Comparison of Scaled GMRS with CSDRS

The scaled horizontal and vertical GMRS are compared to the Westinghouse Certified Seismic Design Response Spectra (CSDRS) on Figure 2.5.2-296. The site scaled GMRS are enveloped by the CSDRS.

Deleted: (Reference 2.5.2-273)

2.5.2.6.6 PBSRS and FIRS

Following the guidance given in Section 5.2.1 of the Interim Staff Guidance DC/COL-ISG-017, a horizontal PBSRS is developed from the design grade UHRS shown on Figure 2.5.2-308 by applying the relationships described in FSAR Subsection 2.5.2.6.3. Figure 2.5.2-309 shows the resulting PBSRS spectra. At frequencies above about 1 Hz the PBSRS is controlled by the 10^{-4} UHRS multiplied by the design factor (DF). At lower frequencies the PBSRS is controlled by 0.45 times the 10^{-5} UHRS.

Section 5.2.1 of the Interim Staff Guidance DC/COL-ISG-017 procedure was then followed to develop SSI input time histories and soil profiles. The first step was to construct a FIRS at the appropriate foundation elevation by extracting ground motions as outcropping motions from the full column site response analyses used to develop the PBSRS. These outcropping motions are used to construct amplification functions that are in turn used to construct a SCOR FIRS for use in developing input time histories. As the site is to be excavated to an elevation of -7 m (-24 ft.) NAVD88 and the reactor placed on approximately 10.7 m (35 ft.) of concrete backfill, the appropriate point for placing the input motion is at the base of the excavation. Therefore, a SCOR FIRS was developed for elevation -7 m (-24 ft.) NAVD88. In addition, a SCOR FIRS was developed at the reactor foundation elevation of +3.3m (+11 ft.) NAVD88 for the purpose of checking the requirement of the minimum level of ground motion specified in 10

Deleted: 4

The SCOR FIRS developed for elevation -7 m (-24 ft.) NAVD88 is shown on Figure 3.7-201. These FIRS have been modified (enhanced) at intermediate frequencies to ensure that the surface response spectra computed using the three site velocity profiles developed for SSI analyses envelop the PBSRS.

2.5.2.6.7 Site Profiles for SSI Analysis

Soil profiles for use in SSI analyses were developed from the PBSRS site response analyses following the requirements of the Standard Review Plan and guidance given in Section 5.2.1 of the Interim Staff Guidance DC/COL-ISG-017. These profiles were based on the statistics of the iterated soil properties for the randomized site profiles used to develop the PBSRS. The best estimate profile was set equal to values interpolated between the median iterated soil properties for the 10^{-4} and 10^{-5} ground motion level input cases using the ratio of the PBSRS peak ground acceleration to the peak acceleration for the 10^{-4} and 10^{-5} UHRS. The resulting site profile is listed in Table 2.5.2-228. The lower bound profile was set equal to the 16th percentile of the distribution of randomized soil properties for the 500 ft/sec engineered fill velocity case, and the upper bound profile was set equal to the 84th percentile of the distribution of randomized soil properties for the 1000 ft/sec engineered fill case. The range in the upper bound and lower bound shear wave velocities was increased where necessary to maintain the minimum coefficient of variation in shear modulus of 1.5. Tables 2.5.2-229 and 2.5.2-230 list the lower bound and upper bound profile properties, respectively. Figure 2.5.2-298 shows the top 500 feet of the three V_s profiles. The corresponding damping ratios were obtained from the statistics of the iterated profiles assuming negative correlation between V_s and damping: that is the 16th percentile damping was used for the upper bound profile and the 84th percentile damping was used for the lower bound profile. The compression wave velocities were based on the measured values for the in-situ materials and the recommend Poisson's ratio of 0.3 for the engineered fill (Table 2.5.4.5-201). The compression wave velocity of water, set to a nominal value of 5000 ft/sec, was used as a minimum value for the compression wave velocities of materials below the water table.

Deleted: GMRS

LNP COL 2.5-3
LNP SUP 3.7-3

A fourth profile called the Lower Lower Bound (LLB) was developed as described in FSAR Subsection 3.7.1.1.1. LLB soil profile is used to account for the degradation of soil shear modulus due foundation installation activities for use in the SSI analysis. The LLB soil profile and properties are shown in Table 2.5.2-231. The degradation of soil shear modulus for the LLB soil profile only applies to in-situ soil layers (layers 7 to 19 in Table 2.5.2-231 which corresponds to depths of 15 ft. to 75 ft.). The material properties for the engineered fill (depths 0 to 15 ft.) and rock (depths greater than 75 ft.) are the same as in the LB soil profile. The low strain shear modulus of the in-situ soil is reduced by 10 percent and the new reduced shear wave velocity was calculated from the shear modulus. The compression wave velocity (V_P) for the in-situ soil was calculated as follows: For in-situ soil below the water table, if the V_P is less than that of water (i.e., 5000 ft/sec), the V_P of the soil is set to 5000 ft/sec (layers 5 to 14 in

Deleted: 4

Table 2.5.2-231). If the V_P is greater than 5000 ft/sec (layer 15 to 19 in Table 2.5.2-231), the V_P is then reduced in the same ratio that the shear wave velocity is being reduced (approximately 5 percent).

2.5.2.7 Sensitivity Evaluations for CEUS SSC

This subsection describes the sensitivity evaluations performed using the CEUS SSC (NUREG-2115) and the modified CAV filter (SECY-2012-0025 Enclosure 7 – Attachment 1 to Enclosure 1) and presents the comparisons of the CEUS hard rock seismic hazards, 10^{-5} finished grade UHRS, GMRS, PBSRS, and FIRS (EL +11 ft.) using the CEUS SSC methodology and those using the updated EPRI SOG methodology scaled to meet 10 CFR Part 50 Appendix S requirements that are presented in Subsection 2.5.2.6.

Deleted: NUREG 2115

Deleted: , Reference 2.5.2-284

2.5.2.7.1 Summary of the CEUS SSC Model

This section summarizes the CEUS SSC model. Details are provided in NUREG-2115. The master logic tree for the CEUS SSC model is shown on Figure 2.5.2-312. The model for seismic sources in the CEUS consists of two types of seismic sources. The first type is seismic source zones used to model future distributed seismicity throughout the CEUS. As shown on Figure 2.5.2-312, two approaches are used to define the distributed seismicity sources. The Mmax Zones approach subdivides the CEUS into regions that are expected to have different values of the maximum magnitude that can occur. The seismotectonic approach subdivides the CEUS into different source zones on the basis of differences in geology and tectonic history. The second type of seismic source is used to model the recurrence of repeated large magnitude earthquakes (RLMEs) that have been identified from the historical and paleoseismic record. The RLME sources are additional sources of large magnitude earthquakes added to the hazard computed from the distributed seismicity sources – either the Mmax source zones or the Seismotectonic source zones. The location of the RLME sources is shown on Figure 2.5.2-313. The nearest RLME source to the LNP site is the Charleston RLME source, which was represented by the UCSS (Reference 2.5.2-243) in the updated EPRI-SOG model used to develop the site seismic hazard results presented in Subsection 2.5.2.4.

The logic tree for the Mmax source zones is shown on Figure 2.5.2-314. There are two interpretations of Mmax zones. The first is that the entire CEUS region is a single source and the second is that the CEUS is divided into two regions, a Mesozoic and younger crustal region (MESE) and an older crustal region (NMESE). There are two interpretations of the boundary between the MESE and NMESE Mmax zones. These are shown on Figures 2.5.2-315 and 2.5.2.316. The LNP site is located in the MESE Mmax source zone.

The logic tree for the Seismotectonic source zones is shown on Figure 2.5.2-317. There are four interpretations of Mmax zones. The two interpretations of the boundary between the MESE and NMESE Mmax zones are used to define alternative boundaries for the Paleozoic Extended Zone (PEZ). In addition, two interpretations are made in for the connection of the Reelfoot Rift with the Rough

Deleted: 4

Creek Graben. The resulting four source zone geometries are shown on Figures 2.5.2-318 through 2.5.2-321. The LNP site is located in the Extended Continental Crust-Gulf Coast (ECC-GC) Seismotectonic source zone.

As shown on Figures 2.5.2-314 and 2.5.2-317, the characterization of the distributed seismicity source zones consists of the use of three alternative magnitude ranges for computing seismicity parameters (Case A, Case B, and Case E), characterization of crustal thickness and rupture geometry, maximum magnitude distributions for each source and seismicity parameter distributions for each source. Seismicity parameters for each source are specified as a set of recurrence rates and *b*-values for individual ¼ degree longitude x ¼ degree latitude or ½ degree longitude x ½ degree latitude cells or partial cells that make up the source area. Uncertainty in the earthquake recurrence parameters is represented in the model by eight alternative sets of these rates and *b*-values – in essence eight alternative maps of predicted future seismicity rates. There are eight alternative sets for each of the three magnitude interval weights (Case A, Case B, and Case E), resulting in a total of 24 alternative sets of earthquake recurrence parameters. The maximum magnitudes for each source zone are represented by a five-point discrete probability distribution that spans a wide range of moment magnitudes. As examples, the maximum magnitude distributions for the source zones that contain the LNP site, the ECC-GC and MESE zones, span the ranges of **M** 6.0 to 8.1 and **M** 6.4 to 8.1, respectively.

The characterization of each of the RLME sources is also in the form of a logic tree. Figure 2.5.2-322 shows the logic tree for the Charleston RLME source. The RLME logic trees address whether or not the RLME is currently active, alternative geometries of the source and of future earthquake ruptures, uncertainty in the average magnitude of future RLMEs, and uncertainty in the recurrence frequency of future RLMEs. The characterization of the Charleston RLME source in the CEUS SSC Model (NUREG-2115) is very similar to the UCSS characterization (Reference 2.5.2-243) that was used to develop the updated EPRI-SOG seismic source model presented in Subsection 2.5.2.4. Comparison of Figures 2.5.2-214 and 2.5.2-322 shows that the uncertainty distributions for maximum (RLME) magnitudes are the same in the two models. The CEUS SSC Charleston RLME source characterization has three alternative models for the geometry of the source. Figure 2.5.2-323 compares these three geometries with the four alternative geometres defined in the UCSS model used in Subsection 2.5.2.4, showing that they cover very similar regions. The recurrence frequency of large earthquakes is also very similar for the two models, being approximately 1.8×10^{-3} earthquakes per year.

Deleted: , Reference 2.5.2-284

2.5.2.7.2 Calculations for the Seven Demonstration Sites

NUREG-2115 presents seismic hazard results computed for seven demonstration sites using the CEUS SSC seismic source model. Figure 2.5.2-324 shows the locations of the demonstration sites relative to the LNP site. Seismic hazard calculations were repeated for these seven sites in order to demonstrate adequate implementation of the CEUS SSC model. These calculations were performed using the seismic source zones used for each site

Deleted: 4

as indicated by the figures presented in Chapter 8 of NUREG-2115 and those RLME sources that had some significant contribution to the hazard at the demonstration sites as indicated by the figures presented in Chapter 8 of NUREG-2115. Hazard calculations were perfomed using the EPRI ground motion models for the CEUS (Reference 2.5.2-253). The hazard from the distributed seismicity source zones was computed using the Cluster 1, Cluster 2, and Cluster 3 models. Earthquakes were modeled as point sources and the EPRI conversions from epicentral distance to rupture distance were used. The hazard from RLME sources was computed using all four of the EPRI Cluster Models and extended earthquake ruptures were explicitly modeled. The updated EPRI models for ground motion variability (Reference 2.5.2-258) were used.

2.5.2.7.2.1 Results for the Central Illinois Site

The source contribution figures presented in Chapter 8 of NUREG-2115 indicate that the source zones used to compute the hazard at the Central Illinois site consist of the seismotectonic sources IBEB, MIDC-A, MIDC-B, MIDC-C, MIDC-D, RR, and RR-RCG; and the Mmax zones MESE-N, MESE-W, NMESE-N, NMESE-W, and the Study_Region. All of these source zones were used in calculation of hazard at the site. The source contribution figures presented in Chapter 8 of NUREG-2115 also indicate that only the New Madrid Faults and the Wabash Valley RLME sources have a contribution to the hazard that would be noticeable in the result and only these two RLME sources were included in the hazard calculations. Figure 2.5.2-325 compares the mean, 5th percentile, 50th percentile, and 85th percentile hazard curves computed in this study with the results listed in Table 8.2.1-1 of NUREG-2115. As shown in the figure the hazard curves computed in this study are close to those presented in NUREG-2115.

2.5.2.7.2.2 Results for the Chattanooga Site

The source contribution figures presented in Chapter 8 of NUREG-2115 indicate that the source zones used to compute the hazard at the Chattanooga site consist of the seismotectonic sources ECC-AM, IBEB, PEZ-N, PEZ-W, MIDC-A, MIDC-B, MIDC-C, MIDC-D, RR, and RR-RCG; and the Mmax zones MESE-N, MESE-W, NMESE-N, NMESE-W, and the Study_Region. All of these source zones were used in calculation of hazard at the site. The source contribution figures presented in Chapter 8 of NUREG-2115 also indicate that only the New Madrid Faults and Charleston RLME sources have a contribution to the hazard that would be noticeable in the result and only these two RLME sources were included in the hazard calculations. Figure 2.5.2-326 compares the mean, 5th percentile, 50th percentile, and 85th percentile hazard curves computed in this study with the results listed in NUREG-2115 Table 8.2.2-1. As shown in the figure the hazard curves computed in this study are close to those presented in NUREG-2115.

2.5.2.7.2.3 Results for the Houston Site

The source contribution figures presented in Chapter 8 of NUREG-2115 indicate that the source zones used to compute the hazard at the Houston site consist of

Deleted: 4

the seismotectonic sources ECC-GC, GHEX, MIDC-A, MIDC-B, MIDC-C, MIDC-D, OKA, RR, and RR-RCG; and the Mmax zones MESE-N, MESE-W, NMESE-N, NMESE-W, and the Study_Region. All of these source zones were used in calculation of hazard at the site. The source contribution figures presented in Chapter 8 of NUREG-2115 also indicate that only the New Madrid Faults and Meers RLME sources have a contribution to the hazard that would be noticeable in the result and only these two RLME sources were included in the hazard calculations. The Gulf Coast versions of the EPRI ground motion models (Reference 2.5.2-253) were used to compute the hazard from all of the seismic sources except the OKA, RR, and RR-RGG source zones and from the Meers and New Madrid RLME sources. Figure 2.5.2-327 compares the mean, 5th percentile, 50th percentile, and 85th percentile hazard curves computed in this study with the results listed in NUREG-2115 Table 8.2.3-1. As shown in the figure the hazard curves computed in this study are close to those presented in NUREG-2115.

Deleted: yyy

2.5.2.7.2.4 Results for the Jackson Site

The source contribution figures presented in Chapter 8 of NUREG-2115 indicate that the source zones used to compute the hazard at the Jackson site consist of the seismotectonic sources ECC-GC, GHEX, MIDC-A, MIDC-B, MIDC-C, MIDC-D, RR, and RR-RCG; and the Mmax zones MESE-N, MESE-W, NMESE-N, NMESE-W, and the Study_Region. All of these source zones were used in calculation of hazard at the site. The source contribution figures presented in Chapter 8 of NUREG-2115 also indicate that only the New Madrid faults, the Marianna zone, and Eastern Rrift Margin South RLME sources have a contribution to the hazard that would be noticeable in the result and only these three RLME sources were included in the hazard calculations. As discussed in Chapter 8 of NUREG-2115, the gulf coast version of the EPRI (2004) ground motion models was used for all sources except those associated with the New Madrid region. Figure 2.5.2-328 compares the mean, 5th percentile, 50th percentile, and 85th percentile hazard curves computed in this study with the results listed in NUREG-2115 Table 8.2.4-1. As shown in the figure the hazard curves computed in this study are close to those presented in NUREG-2115.

2.5.2.7.2.5 Results for the Manchester Site

The source contribution figures presented in Chapter 8 of NUREG-2115 indicate that the source zones used to compute the hazard at the Manchester site consist of the seismotectonic sources ECC-AM, MIDC-A, MIDC-C, PEZ-N, PEZ-W, NAP, and SLR; and the Mmax zones MESE-N, MESE-W, NMESE-N, NMESE-W, and Study_Region. All of these source zones were used in calculation of hazard at the site. The source contribution figures presented in Chapter 8 of NUREG-2115 also indicate that only the Charlevoix RLME source has a contribution to the hazard that would be noticeable in the result and only this RLME sources were included in the hazard calculations. Figure 2.5.2-329 compares the mean, 5th percentile, 50th percentile, and 85th percentile hazard curves computed in this study with the results listed in NUREG-2115 Table 8.2.5-1. As shown in the

Deleted: 4

figure the hazard curves computed in this study are close to those presented in NUREG-2115.

2.5.2.7.2.6 Results for the Savannah Site

The source contribution figures presented in Chapter 8 of NUREG-2115 indicate that the source zones used to compute the hazard at the Savannah site consist of the seismotectonic sources AHEX, ECC-AM, ECC-GC, PEZ-N, and PEZ-W; and the Mmax zones MESE-N, MESE-W, NMESE-N NMESE-W, and Study_region. All of these source zones were used in calculation of hazard at the site. The source contribution figures presented in Chapter 8 of NUREG-2115 also indicate that only the Charleston RLME source has a contribution to the hazard that would be noticeable in the result and only this RLME sources were included in the hazard calculations. The initial implementation of the Charleston RLME followed that used for the UCSS (Reference 2.5.2-243) described in Subsection 2.5.2.4.3.3. The Regional and Local geometries were modeled by a series of closely spaced pseudo faults parallel to the northeast orientation of the zone and earthquake ruptures were modeled as occurring uniformly along these faults. This process produced acceptable results at the Chattanooga site, but underestimated the hazard from this source at Savannah. An alterntive approach was used in which the source zone was filled with a grid of uniformly spaced points. At each location, magnitude-dependent ruptures were placed with the specified northeast orientation with a random location on the grid point. The "strict" boundary condition for the Regional and Local geometries was then imposed by forcing the ruptures to remain within the source boundary. The net effect of this model is to increase the probability of rupture locations near the boundary compared to the assumption of a uniform distribution of rupture within the source. This alternative process produced acceptable results. Figure 2.5.2-330 compares the mean, 5th percentile, 50th percentile, and 85th percentile hazard curves computed in this study with the results listed in NUREG-2115 Table 8.2.6-1. These results show greater differences for the Savannah site between the hazard curves computed in this study and those presented in NUREG-2115 compared to the other six demonstration sites. These differences are likely due to differences in the details of modeling the RLME rupture geometries at distances close to the site. However, these differences in modeling have minimal impact on the computation of mean hazard at large distances from the Charleston RLME soruce, as evidenced by the ability to reproduce the hazard at the Chattanooga site. Thus, the differences in modeling are not significant to the hazard at the LNP site, which is also at a large distance from the Charleston RLME source.

2.5.2.7.2.7 Results for the Topeka Site

The source contribution figures presented in Chapter 8 of NUREG-2115 indicate that the source zones used to compute the hazard at the Topeka site consist of the seismotectonic sources MIDC-A, MIDC-B, MIDC-C, and MIDC-D; and the Mmax zones NMESE-N, NMESE-W, and Study_Region. All of these source zones were used in calculation of hazard at the site. The source contribution figures presented in Chapter 8 of NUREG-2115 also indicate that only the New

Deleted: 4

Madrid Faults and Meers RLME sources have a contribution to the hazard that would be noticeable in the result and only this RLME sources were included in the hazard calculations. Figure 2.5.2-331 compares the mean, 5th percentile, 50th percentile, and 85th percentile hazard curves computed in this study with the results listed in NUREG-2115 Table 8.2.7-1. As shown in the figure the hazard curves computed in this study are close to those presented in NUREG-2115.

2.5.2.7.2.8 Summary if Results of Calculations for the Demonstration Sites

The comparison plots shown on Figures 2.5.2-325 through 2.5.2-331 show that the implementation of the CEUS SSC model using AMEC E&I software is able to closely match the mean and fractile hazard curves at the demonstration sites. The mean hazard curves listed in Tables 8.2.1-1 through 8.2.7-1 of NUREG-2115 and computed in this study were used to compute ground motion levels with annual exceedance frequencies of 10^{-4}, 10^{-5}, and 10^{-6}. These results are listed in Table 2.5.2-232. The differences in the ground motion values are generally less than 5 percent. As discussed in Chapter 9 of NUREG-2115, this difference in mean ground motion levels is not considered a significant difference. Therefore, it is concluded the implementation of the CEUS SSC model for this study is adequate for the purpose of computing hazard at the LNP site.

Deleted: ¶

The one case where larger differences were obtained is for the Savannah site. The larger differences at this site are attributed to differences in the details of modeling of large magnitude rupture locations for sites near the source. At the Chattanooga site, the hazard from the Charleston RLME source computed in this study using the implementation uniform rupture locations on pseudo faults produced hazard results that were comparable to those shown in Chapter 8 of NUREG-2115. Thus, it is expected that differences in the details of modeling the geometry of RLME ruptures in the Charleston source will have little impact on the calculated hazard at distant sites, such as the LNP site.

2.5.2.7.3 Calculation of Hard Rock Hazard at the LNP Site Using the CEUS SSC Model

This section presents the results of calculations of the hard hazard at the LNP site using the CEUS SSC model.

Deleted: ¶

2.5.2.7.3.1 Implementation of the CEUS SSC Model for the LNP Site

The hazard calculations using the CEUS SSC model included contributions from all distributed seismicity source zones that extend within 1,000 km of the LMP site. Figures 2.5.2-315 and 2.5.2-316 show the location of the LNP site relative to the Mmax source zones. All the Mmax source zones were included in the calculations for the LNP site: MESE-N, MESE-W, NMESE-N, NMESE-W, and the Study_Region. Figures 2.5.2-318 through 2.5.2-321 show the location of the LNP site relative to the Seismotectonic source zones. The Seismotectonic source zones included in the hazard calculation are AHEX, GHEX, ECC-AM, ECC-GC,

Deleted: 4

MIDC (-A, -B, -C, and –D), PEZ (-N and –W), RR and RR-RCG. Figure 2.5.2-313 shows the location of the LNP site relative to the RLME sources. The Charleston and New Madrid Faults RLME sources were included in the hazard calculations. The other RLME sources near the New Madrid faults were not included based on their low contribution to the hazard at Chattanooga shown in Chapter 8 of NUREG-2115 and the greater distance to the LNP site. Because the LNP site is at a large distance from the Charleston RLME source, difference in the details of the implementation of rupture geometries for this source are unimportant, as demonstrated by the ability to match the hazard results at Chattanooga.

Deleted: ¶

Deleted: ¶

Hazard calculations were perfomed using the EPRI ground motion models for the CEUS (Reference 2.5.2-253). Following the procedure used for the hazard based on the updated EPRI-SOG model described in Subsection 2.5.2.4.4 and for the CUES SSC model demonstration site calculations described in Subsection 2.5.2.7.2, the hazard from the distributed seismicity source zones was computed using the EPRI Cluster 1, Cluster 2, and Cluster 3 models. Earthquakes were modeled as point sources and the EPRI conversions from epicentral distance to rupture distance were used. The hazard from RLME sources was computed using all four of the EPRI Cluster Models and extended earthquake ruptures were explicitly modeled. The updated EPRI models for ground motion variability (Reference 2.5.2-258) were used. Consistent with the calculations using the updated EPRI-SOG model, the the Gulf Coast version of the EPRI CEUS ground motion models were used for the site host zone, ECC-GC and the GHEX source. These models were also used for the RR and RR-RCG source zones and the New Madrid RLME source as nearly all of the travel path from these sources to the LNP site is through the Gulf Coast attenuation region defined in Reference 2.5.2-260 (see for example Figure 2.5.2-204).

Hazard calculations were performed using a minimum magnitude of **M** 5.0, consistent with the recommendations in SECY-2012-0025 (Enclosure 7 – Attachment 1 to Enclosure 1). Because the earthquake recurrence rates and maximum magnitudes for all sources in the CEUS SSC model are defined in terms of the moment magnitude scale **M**, the magnitude conversion relationships between m_b and **M** described in Subsection 2.5.2.4.2.3 are not needed to perform the hazard calculation.

Deleted: ¶

2.5.2.7.3.2 Hard Rock Hazard Results for the LNP Site

Hazard calculations were performed for the seven spectral frequencies for which the EPRI (Reference 2.5.2-253) ground motion models are defined: 0.5, 1.0, 2.5, 5.0, 10.0, 25.0 Hz, and PGA (100 Hz). Figures 2.5.2-332 through 2.5.2-338 compare the mean and fractiles hazard curves based on the updated EPRI-SOG model (Figures 2.5.2-226 through 2.5.2-232) with those computed using the CEUS SSC model. The comparisons show that the rock hazard based on the CEUS SSC model is similar to that obtained based on the updated EPRI-SOG model for spectral frequencies of 2.5 Hz and lower and is somewhat lower for higher spectral frequencies.

Figure 2.5.2-339 shows the contributions from the two main source types – distributed seismicity and the Charleston source - to the total mean hazard for 10

Deleted: ¶

Deleted: 4

Hz and 1 Hz. The results indicate that the CEUS SSC Charleston RLME source produces hazard that is slightly less than that produced by the Charleston source (UCSS) used in the updated EPRI-SOG model presented in Subsection 2.5.2.4. As discussed above in Subsection 2.5.2.7.1, the UCSS and Charleston RLME sources have the same maximum magnitude distribution, nearly identical mean recurrence frequencies and nearly the same minimum distance from the LNP site. The difference in hazard is attributed primarily to differences in the implementation of the recurrence model in the two calculations. The Charleston RLME source models the size of future earthquakes using five alternative values of the expected magnitude of the repeated large magnitude earthquakes, as shown on Figures 2.5.2-214 and 2.5.2-322. For each value of the expected magnitude values, the size of individual earthquakes is modeled as uniformly distributed over the range of ±0.25 magnitude units about the expected magnitude. The implementation of the UCSS model in the updated EPRI-SOG model presented in Subsection 2.5.2.4 converted the expected magnitudes in terms of **M** to m_b for consistency in combining with the hazard from the EPRI-SOG sources. In that implementation the magnitude distribution was implemented as ±0.25 m_b magnitude units. These were converted back to **M** for the purpose of computing ground motions using the relationships given in Subsection 2.5.2.4.2.3. As a result, the effective moment magnitudes at the upper end of the magnitude ranges are larger than the corresponding values in the Charleston RLME source by 0.12 to 0.26 moment magnitude units. These somewhat larger magnitudes are the likely reason for the slightly larger hazard computed for the UCSS source compared to that computed for the Charleston RLME.

The results shown on Figure 2.5.2-339 show that the 10 Hz hazard from the CEUS SSC model for distributed seismicity is somewhat lower than that from the updated EPRI-SOG sources. This indicates that the CEUS SSC model predicts somewhat lower seismicity rates in the region around the LNP site compared to the updated EPRI-SOG model. For 1 Hz hazard, the hazard from the distributed seismicity sources in the CEUS SSC model is higher than the hazard from the updated EPRI-SOG distributed seismicity sources. This higher hazard at 1 Hz is likely due to the larger maximum magnitudes for the CEUS SSC source zones compared to those for the updated EPRI-SOG source zones. However, the hazard at low frequencies is dominated by the Charleston RLME for exceedance frequencies of 10^{-4} to 10^{-5} such that the higher hazard from the distributed seismicity sources does not lead to an increase in total hazard.

Deleted: ¶

The mean seismic hazard curves for the LNP site computed using the CEUS SSC model are used to obtain hard rock UHRS. Figure 2.5.2-340 compares the hard rock UHRS based on the CEUS SSC model to those based on the updated EPRI-SOG model (shown on Figure 2.5.2-238). The hard rock UHRS based ont the CEUS-SSC model are somewhat lower than those based on the updated EPRI-SOG model at spectral frequencies above 2.5 Hz and are similar for lower spectral frequencies. The only place where the CEUS SSC model produces higher motions is for the 10^{-3} UHRS at low frequencies. This higher hazard is again likely due to the larger maximum magnitudes for the distributed seismicity sources in the CEUS SSC model.

Deleted: 4

2.5.2.7.3.3 Deaggregation of Hard Rock Hazard Results Based on the CEUS SSC Model

The rock hazard results for 1, 2.5, 5, and 10 Hz computed using the CEUS SSC model were deaggregated to compare with the deaggregation results from the updated EPRI-SOG model presented in Subsection 2.5.2.4.4.2. As described in Subsection 2.5.2.4.4.2, the deaggregation was performed following the guidance presented in Appendix D of US NRC Regulatory Guide 1.208. Figures 2.5.2-341, 2.5.2-342, 2.5.2-343, and 2.5.2-344 show the deaggregation results for mean annual exceedance frequencies of 10^{-3}, 10^{-4}, 10^{-5} and 10^{-6}, respectively. These deaggregation results are generally similar to those for the updated EPRI-SOG hazard results shown on Figures 2.5.2-239 through 2.5.2-242. The hazard at the LNP site is the result of a mixure of contributions from moderate magnitude earthquakes at a range of distances around the site and large earthquakes occurring at distances of 400 to 500 km associated with the Charleston RLME source.

The hazard deaggregation results presented on Figures 2.5.2-341 through 2.5.2-344 were used to develop reference (controlling) earthquakes (REs) and deaggregation earthquakes (DEs) in the same manner as presented in Subsection 2.5.2.4.4.2. The DE and RE magnitudes and distances are listed on the left hand side of Table 2.5.2-233. The right hand side of Table 2.5.2-233 lists the RE and DE magnitudes and distances based on the updated EPRI-SOG model from Table 2.5.2-221. The deaggregation results from the two source models are generally similar. The magnitudes for updated EPRI-SOG model hazard results are given in terms of m_b while those for the CEUS SSC hazard results are given in terms of **M**. Thus, the magnitudes for the CEUS SSC hazard results are expected to be somewhat larger based on the magnitude conversions between m_b and **M** described in Subsection 2.5.2.4.2.3.

2.5.2.7.4 Calculation of GMRS, PBSRS, and FIRS at the LNP Site Using the CEUS SSC Model with Modified CAVI

This section presents the calculation of the GMRS, PBSRS and FIRS for the LNP site using the CEUS SSC model with the modifications to the application of CAV specified in SECY-2012-0025 (Enclosure 7 – Attachment 1 to Enclosure 1). These ground motion spectra are compared to those developed using the updated EPRI-SOG model presented in Subsection 2.5.2.6.

2.5.2.7.4.1 Inputs to the Calculation of the GMRS and PBSRS Using the the CEUS SSC Model and Modified CAV

The seismic source inputs from the CEUS SSC model used for calculation of the hazard with CAV are the same as those used for calculation of the hard rock hazard presented in section 2.5.2.7.3, with the exception that the hazard integration uses a minimum magnitude of **M** 4.0 and the earthquake recurrence parameters used are those developed for magnitude **M** 4.0 and larger earthquakes. Following the guidance given in SECY-2012-0025 (Enclosure 7 –

Attachment 1 to Enclosure 1), application of the CAV filte was limited to magnitudes less than **M** 5.5.

Calculation of the hazard at the GMRS and PBSRS elevations requires the useof site amplification functions. Subsections 2.5.2.5.3.1 and 2.5.2.5.3.2 present the development of site amplification functions for the GMRS and PBSRS profiles, respectively. These amplification functions were developed using Approach 2B of NUREG/CR-6728 (Reference 2.5.2- 263) in which site response analyses were conducted using input ground motion time histories developed to match on average the response spectra for the deaggregation earthquakes (DEs) listed in Table 2.5.2-221. As discussed in Subsection 2.5.2.7.3.3, the deaggregation of the hard rock hazard computed using the CEUS SSC model is generally similar to that obtained for the updated EPRI-SOG model and leads to similar RE and DE magnitudes and distances, as shown in Table 2.5.2-233. Furthermore, the site amplification functions developed for the GMRS profile shown on Figure 2.5.2-272 are nearly the same for all three DE inputs for frequencies of below about 20 Hz and the high frequency (HF) amplification function shows relatively low sensitivity to the alternative DE earthquakes at higher frequencies. Therefore, the relatively small differences in relative weights assigned to the DEs (Table 2.5.2-233) are not expected to produce large changes in the mean amplification functions. Thus, the existing site amplification functions are considered adequate for the purpose of computing the CAV hazard based on the CEUS SSC model for comparison with the hazard results based on the updated EPRI-SOG model.

2.5.2.7.4.2 Seismic Hazard Results for the CEUS SSC Model and Modified CAV

Figures 2.5.2-345 through 2.5.2-351 compare the mean and fractiles hazard computed using the CEUS SSC model with those based on the updated EPRI-SOG model presented in Figures 2.5.2-286 through 2.5.2-292 for the GMRS profile and Figures 2.5.2-301 through 2.5.2-307 for the PBSRS profiles. These figures show the influence of the restriction of application of the EPRI CAV model (Reference 2.5.2-280) to only earthquakes with magnitudes < **M** 5.5. Instead of leveling off at a specific exceedance frequency at low ground motions levels, the CAV hazard curves continue to rise as the ground motion level decreases, following the trend of the nonCAV hard rock hazard curves. As a result, the modification to the application of the CAV model has a significant effect on the resulting 10^{-4} ground motions interpolated from the mean hazard curves, which results in higher ground motions at the 10^{-4} exceedance level. At 10^{-5} and lower exceedance frequencies the effect of the modification in the application of the CAV model is much less as the CAV and nonCAV hazard curves have the same trend and the difference in the CAV hazard curves between the previous calculations based on the updated EPRI-SOG model and the results based on the CEUS SSC model reflects the difference in hard rock hazard.

Figures 2.5.2-352 and 2.5.2-353 show the computed UHRS for the GMRS and PBSRS elevations, respectively. The solid curves show the UHRS based on the

Deleted: 4

updated EPRI-SOG model with full CAV and the dashed show the UHRS based on the CEUS SSC model and the modified CAV application. Note that the 10^{-4} UHRS for the GMRS elevation is undefined for the updarted EPRI-SOG model because the mean CAV hazard curve lies below 10^{-4} exceedance frequency.

The results for the GMRS elevation show that the 10^{-4} and 10^{-5} UHRS based on the CEUS SSC model and revised CAV application are higher than those based on the updated EPRI-SOG model with full CAV. The higher motions are due primarily to the modification to the application of the EPRI CAV model. The results for the PBSRS elevation show that the 10^{-4} UHRS based on the CEUS SSC model and revised CAV application is higher than the 10^{-4} UHRS based on the updated EPRI-SOG model with fill CAV while the 10^{-5} and 10^{-6} UHRS amplitudes are similar for frequencies of 5 Hz and less and lower at higher spectral frequencies. The higher 10^{-4} UHRS is again due primarily to the change in the application of the CAV. The lower 10^{-5} and 10^{-6} UHRS amplitudes at spectral frequencies above 5 Hz are due to the difference in the rock hazard between the two models.

2.5.2.7.4.3 GMRS based on CEUS SSC Model and Modified CAV

The GMRS based on hazard results computed using the CEUS SSC model and modified CAV are developed using a similar approach to that used in Subsection 2.5.2.6 to develop the GMRS based on the updated EPRI-SOG model. Subsection 2.5.2.6.1 presents the development of smooth horizontal UHRS for the GMRS elevation based on hazard results computed without CAV using the updated EPRI-SOG model. These UHRS are shown on Figure 2.5.2-293. Subsection 2.5.2.6.2 describes the development of CAV/nonCAV response spectral ratios for the seven spectral frequencies of 0.5, 1, 2.5, 5, 10, 25, and 100 Hz contained in the EPRI ground motion models. These spectral ratios were interpolated to cover the frequency range of 0.1 to 100 Hz and the interpolated spectral ratios were used to scale the nonCAV UHRS to produce CAV UHRS. The same process is used to produce smooth horizontal UHRS based on the CEUS SSC model with modified CAV. The GMRS elevation UHRS amplitudes at the seven spectral frequencies computed using the CEUS SSC model with modified CAV (Figure 2.5.2-352) are divided by the UHRS amplitudes computed using the updated EPRI-SOG UHRS without CAV to produce a new set of spectral ratios. These spectral ratios are then used to scale the nonCAV smooth horizontal UHRS presented in Subsection 2.5.2.6.1 to produce smooth horizontal UHRS based on the CEUS SSC model and modified CAV. The resulting 10^{-4} and 10^{-5} UHRS are shown on Figure 2.5.2-354. The relationships given in Regulatory Guide 1.208 and described in Subsection 2.5.2.6.3 are then used to compute the GMRS from the 10^{-4} and 10^{-5} UHRS. Two spectra are computed, one based on the design factors (DF) computed using Equations 2.5.2-216 and 2.5.2-217 and one equal to 0.45 times the 10^{-5} UHRS. These two spectra are shown on Figure 2.5.2-354. The GMRS is the envelope of these two spectra. The third column of Table 2.5.2-234 lists the resulting horizontal GMRS.

The vertical GMRS based on the CEUS SSC model with modified CAV is computed from the horizontal GMRS using the vertical to horizontal spectral

Deleted: 4

ratios (V/H) developed in Subsection 2.5.2.6.4 and listed in Table 2.5.2-226. Those spectral ratios are appropriate for uses because the peak acceleration of the GMRS remains less that 0.2g. The resulting vertical GMRS is listed in the sixth column of Table 2.5.2-234. Figure 2.5.2-355 compares the GMRS based on the CEUS SSC model with modified CAV to the scaled GMRS based on the updated EPRI-SOG model with full CAV. The percent differences between the two sets of GMRS are given in Table 2.5.2-234. The GMRS based on the CEUS SSC model with modified CAV is enveloped by the GMRS based on the updated EPRI-SOG model with full CAV except for frequencies between 0.2 and 2 Hz where the CEUS SSC based GMRS is up to 4 percent higher. Both sets of GMRS are well enveloped by the Westinghouse AP1000 CSDRS.

Deleted: ¶
¶

2.5.2.7.4.4 PBSRS and FIRS based on CEUS SSC Model and Modified CAV

The PBSRS based on hazard results computed using the CEUS SSC model and modified CAV are developed using a similar approach to that used in Subsection 2.5.2.7.4.3 for the GMRS. The PBSRS elevation UHRS amplitudes at the seven spectral frequencies computed using the CEUS SSC model with modified CAV (Figure 2.5.2-353) are divided by the UHRS amplitudes computed using the updated EPRI-SOG UHRS without CAV to produce a new set of spectral ratios. These spectral ratios are then used to scale the nonCAV smooth horizontal UHRS presented in Subsection 2.5.2.6.6 to produce smooth horizontal UHRS based on the CEUS SSC model and modified CAV. The resulting 10^{-4} and 10^{-5} UHRS are shown on Figure 2.5.2-356. The relationships given in Regulatory Guide 1.208 and described in Subsection 2.5.2.6.3 are then used to compute the PBSRS from the 10^{-4} and 10^{-5} UHRS. Two spectra are computed, one based on the design factors (DF) computed using Equations 2.5.2-216 and 2.5.2-217 and one equal to 0.45 times the 10^{-5} UHRS. These two spectra are shown on Figure 2.5.2-356. The PBSRS is the envelope of these two spectra. The third column of Table 2.5.2-235 lists the resulting horizontal PBSRS.

The vertical PBSRS based on the CEUS SSC model with modified CAV is computed from the horizontal PBSRS using the vertical to horizontal spectral ratios (V/H) developed in Subsection 2.5.2.6.6 and listed in Table 2.5.2-227. Those spectral ratios are appropriate for uses because the peak acceleration of the PBSRS remains less than 0.2g. The resulting vertical PBSRS is listed in the sixth column of Table 2.5.2-235.

Figure 2.5.2-357 compares the PBSRS based on the CEUS SSC model with modified CAV to the scaled PBSRS based on the updated EPRI-SOG model with full CAV. The percent differences between the two sets of GMRS are given in Table 2.5.2-235. The PBSRS based on the CEUS SSC model with modified CAV is enveloped by the PBSRS based on the updated EPRI-SOG model with full CAV. Both sets of PBSRS are well enveloped by the Westinghouse AP1000 CSDRS.

The Reactor Building FIRS based on the CEUS SSC model with modified CAV are computed in a similar manner using the spectral ratios of the UHRS at the

Deleted: ¶

Deleted: 4

PBSRS elevation computed using the CEUS SSC model with modified CAV divided by the UHRS amplitudes computed using the updated EPRI-SOG UHRS without CAV. Figure 2.5.2-358 compares the FIRS based on the CEUS SSC model with modified CAV to the scaled FIRS based on the updated EPRI-SOG model with full CAV. The FIRS based on the CEUS SSC model with modified CAV are enveloped by the scaled FIRS based on the updated EPRI-SOG model with full CAV.

Deleted: ¶

2.5.2.7.5 Summary of the Results of Sensitivity Analyses Using the CEUS SSC Model

Comparisons between the scaled GMRS, PBSRS, and FIRS developed using the updated EPRI-SOG model with full CAV and the corresponding spectra developed using the CEUS SSC model with modified CAV are provided are shown on Figures 2.5.2-355, 2.5.2-357, and 2.5.2-358. These comparisons show that the PBSRS and FIRS based on the CEUS SSC model with modified CAV are enveloped by the corresponding spectra developed using the updated EPRI-SOG model with full CAV. The GMRS based on the CEUS SSC model with modified CAV is also nearly enveloped by the scaled GMRS based on the updated EPRI-SOG model with full CAV, with the maximum exceedance being 4 percent near 1 Hz. Thus, it is concluded that the site specific ground motions developed using the updated EPRI-SOG model with full CAV presented in Subsection 2.5.2.6 are appropriate for use as the design basis for the LNP site.

Deleted: in Tables 2.5.2-234 and 2.5.2-235 and

Deleted: ¶
¶

Levy Nuclear Plant Units 1 and 2
COL Application
Part 2, Final Safety Analysis Report

LNP COL 2.5-3

Table 2.5.2-226
LNP Site GMRS Scaled by 1.2121 consistent with Reactor Foundation Elevation SCOR FIRS Scaled to 0.1g Horizontal Peak Ground Acceleration
(Sheet 1 of 2)

Spectral Frequency (Hz)	5 Percent Damped Spectral Acceleration (g)			
	10^{-5} UHRS	Horizontal Scaled GMRS	Vertical/Horizontal	Vertical Scaled GMRS
100.000	0.1537	0.0838	0.744	0.0624
60.241	0.1889	0.1031	0.762	0.0786
50.000	0.2144	0.1170	0.799	0.0934
40.000	0.2396	0.1307	0.874	0.1142
33.333	0.2621	0.1430	0.900	0.1286
30.303	0.2717	0.1482	0.894	0.1325
25.000	0.3163	0.1726	0.869	0.1500
23.810	0.3250	0.1773	0.860	0.1526
22.727	0.3335	0.1820	0.850	0.1547
21.739	0.3419	0.1865	0.840	0.1567
20.833	0.3500	0.1910	0.827	0.1579
20.000	0.3580	0.1954	0.815	0.1591
18.182	0.3755	0.2049	0.784	0.1606
16.667	0.3922	0.2140	0.755	0.1615
15.385	0.4081	0.2227	0.732	0.1630
14.286	0.4235	0.2311	0.714	0.1649
13.333	0.4383	0.2392	0.697	0.1668
12.500	0.4527	0.2470	0.682	0.1684
11.765	0.4610	0.2515	0.668	0.1680
11.111	0.4634	0.2528	0.655	0.1655
10.526	0.4657	0.2541	0.642	0.1631
10.000	0.4679	0.2553	0.630	0.1608
9.091	0.4725	0.2578	0.619	0.1596
8.333	0.4767	0.2601	0.614	0.1598
7.692	0.4635	0.2529	0.610	0.1542
7.143	0.4515	0.2464	0.606	0.1492
6.667	0.4407	0.2405	0.602	0.1447
6.250	0.4317	0.2355	0.600	0.1413
5.882	0.4233	0.2310	0.600	0.1386
5.556	0.4156	0.2268	0.600	0.1361
5.263	0.4085	0.2229	0.600	0.1337
5.000	0.4018	0.2192	0.600	0.1315
4.545	0.3870	0.2111	0.600	0.1267
4.167	0.3740	0.2040	0.600	0.1224
3.846	0.3624	0.1977	0.600	0.1186
3.571	0.3519	0.1920	0.600	0.1152
3.333	0.3425	0.1869	0.600	0.1121
3.125	0.3339	0.1822	0.600	0.1093
2.941	0.3260	0.1779	0.600	0.1067
2.778	0.3188	0.1739	0.600	0.1044
2.632	0.3121	0.1703	0.600	0.1022
2.500	0.3058	0.1669	0.600	0.1001
2.381	0.2993	0.1633	0.600	0.0980
2.273	0.2933	0.1600	0.600	0.0960
2.174	0.2876	0.1569	0.600	0.0941
2.083	0.2822	0.1540	0.600	0.0924
2.000	0.2772	0.1512	0.600	0.0907
1.818	0.2658	0.1450	0.600	0.0870

Rev. 5

Deleted: 0.0691 ... [1]
Deleted: 0.0838 ... [2]
Deleted: 0.0965 ... [3]
Deleted: 0.1078 ... [4]
Deleted: 0.1180 ... [5]
Deleted: 0.1223 ... [6]
Deleted: 0.1423 ... [7]
Deleted: 0.1463 ... [8]
Deleted: 0.1501 ... [9]
Deleted: 0.1538 ... [10]
Deleted: 0.1575 ... [11]
Deleted: 0.1611 ... [12]
Deleted: 0.1690 ... [13]
Deleted: 0.1765 ... [14]
Deleted: 0.1837 ... [15]
Deleted: 0.1906 ... [16]
Deleted: 0.1973 ... [17]
Deleted: 0.2037 ... [18]
Deleted: 0.2075 ... [19]
Deleted: 0.2085 ... [20]
Deleted: 0.2096 ... [21]
Deleted: 0.2105 ... [22]
Deleted: 0.2126 ... [23]
Deleted: 0.2145 ... [24]
Deleted: 0.2086 ... [25]
Deleted: 0.2032 ... [26]
Deleted: 0.1983 ... [27]
Deleted: 0.1943 ... [28]
Deleted: 0.1905 ... [29]
Deleted: 0.1870 ... [30]
Deleted: 0.1838 ... [31]
Deleted: 0.1808 ... [32]
Deleted: 0.1741 ... [33]
Deleted: 0.1683 ... [34]
Deleted: 0.1631 ... [35]
Deleted: 0.1584 ... [36]
Deleted: 0.1541 ... [37]
Deleted: 0.1503 ... [38]
Deleted: 0.1467 ... [39]
Deleted: 0.1435 ... [40]
Deleted: 0.1404 ... [41]
Deleted: 0.1376 ... [42]
Deleted: 0.1347 ... [43]
Deleted: 0.1320 ... [44]
Deleted: 0.1294 ... [45]
Deleted: 0.1270 ... [46]
Deleted: 0.1247 ... [47]
Deleted: 0.1196 ... [48]
Deleted: 4

LNP COL 2.5-3

Table 2.5.2-226
LNP Site GMRS Scaled by 1.2121 consistent with Reactor Foundation Elevation SCOR FIRS Scaled to 0.1g Horizontal Peak Ground Acceleration
(Sheet 2 of 2)

Spectral Frequency (Hz)	5 Percent Damped Spectral Acceleration (g)			
	10^{-5} UHRS	Horizontal Scaled GMRS	Vertical/Horizontal	Vertical Scaled GMRS
1.667	0.2558	0.1396	0.600	0.0837
1.538	0.2451	0.1337	0.600	0.0802
1.429	0.2317	0.1264	0.600	0.0758
1.333	0.2199	0.1200	0.600	0.0720
1.250	0.2062	0.1125	0.600	0.0675
1.176	0.1941	0.1059	0.600	0.0636
1.111	0.1834	0.1001	0.600	0.0600
1.053	0.1738	0.0948	0.600	0.0569
1.000	0.1652	0.0901	0.600	0.0541
0.909	0.1548	0.0845	0.600	0.0507
0.833	0.1460	0.0796	0.600	0.0478
0.769	0.1383	0.0754	0.600	0.0453
0.714	0.1315	0.0718	0.600	0.0431
0.667	0.1255	0.0685	0.600	0.0411
0.625	0.1201	0.0655	0.600	0.0393
0.588	0.1153	0.0629	0.600	0.0377
0.556	0.1109	0.0605	0.600	0.0363
0.526	0.1069	0.0583	0.600	0.0350
0.500	0.1033	0.0564	0.600	0.0338
0.455	0.0893	0.0487	0.600	0.0292
0.417	0.0781	0.0426	0.600	0.0256
0.385	0.0691	0.0377	0.600	0.0226
0.357	0.0617	0.0337	0.600	0.0202
0.333	0.0555	0.0303	0.600	0.0182
0.313	0.0505	0.0275	0.600	0.0165
0.294	0.0461	0.0252	0.600	0.0151
0.278	0.0425	0.0232	0.600	0.0139
0.263	0.0393	0.0214	0.600	0.0129
0.250	0.0365	0.0199	0.600	0.0119
0.238	0.0341	0.0186	0.600	0.0112
0.227	0.0319	0.0174	0.600	0.0104
0.217	0.0299	0.0163	0.600	0.0098
0.208	0.0282	0.0154	0.600	0.0092
0.200	0.0266	0.0145	0.600	0.0087
0.182	0.0232	0.0127	0.600	0.0076
0.167	0.0206	0.0112	0.600	0.0067
0.154	0.0183	0.0100	0.600	0.0060
0.143	0.0165	0.0090	0.600	0.0054
0.133	0.0149	0.0081	0.600	0.0049
0.125	0.0136	0.0074	0.600	0.0044
0.118	0.0124	0.0068	0.600	0.0041
0.111	0.0114	0.0062	0.600	0.0037
0.100	0.0097	0.0053	0.600	0.0032

Notes:

Hz = hertz

Deleted: 0.1043 ... [1]
Deleted: 0.0989 ... [2]
Deleted: 0.0928 ... [3]
Deleted: 0.0874 ... [4]
Deleted: 0.0825 ... [5]
Deleted: 0.0782 ... [6]
Deleted: 0.0743 ... [7]
Deleted: 0.0697 ... [8]
Deleted: 0.0657 ... [9]
Deleted: 0.0622 ... [10]
Deleted: 0.0592 ... [11]
Deleted: 0.0565 ... [12]
Deleted: 0.0541 ... [13]
Deleted: 0.0519 ... [14]
Deleted: 0.0499 ... [15]
Deleted: 0.0481 ... [16]
Deleted: 0.0465 ... [17]
Deleted: 0.0402 ... [18]
Deleted: 0.0352 ... [19]
Deleted: 0.0311 ... [20]
Deleted: 0.0278 ... [21]
Deleted: 0.0250 ... [22]
Deleted: 0.0227 ... [23]
Deleted: 0.0207 ... [24]
Deleted: 0.0191 ... [25]
Deleted: 0.0177 ... [26]
Deleted: 0.0164 ... [27]
Deleted: 0.0153 ... [28]
Deleted: 0.0144 ... [29]
Deleted: 0.0135 ... [30]
Deleted: 0.0127 ... [31]
Deleted: 0.0120 ... [32]
Deleted: 0.0105 ... [33]
Deleted: 0.0092 ... [34]
Deleted: 0.0082 ... [35]
Deleted: 0.0074 ... [36]
Deleted: 0.0067 ... [37]
Deleted: 0.0061 ... [38]
Deleted: 0.0056 ... [39]
Deleted: 0.0051 ... [40]
Deleted: 0.0044 ... [41]
Deleted: 4

Rev. 5

Table 2.5.2-232: Comparison of Ground Motions Computed from Mean Hazard Curves for the Seven Demonstration Sites

Demonstration Site	Ground Motion Parameter	Ground Motion Level (g)		Percent Difference
		This Calculation	NUREG-2115 Chapter 8	
Central Illinois	10^{-4} PGA	0.183	0.178	2.5%
	10^{-5} PGA	0.611	0.581	5.2%
	10^{-6} PGA	1.691	1.613	4.8%
	10^{-4} 10 Hz PSA	0.365	0.357	2.0%
	10^{-5} 10 Hz PSA	1.113	1.070	4.0%
	10^{-6} 10 Hz PSA	2.952	2.831	4.3%
	10^{-4} 1 Hz PSA	0.108	0.106	2.2%
	10^{-5} 1 Hz PSA	0.246	0.240	2.6%
	10^{-6} 1 Hz PSA	0.507	0.495	2.5%
Chattanooga	10^{-4} PGA	0.338	0.329	2.7%
	10^{-5} PGA	1.113	1.086	2.5%
	10^{-6} PGA	2.592	2.537	2.2%
	10^{-4} 10 Hz PSA	0.624	0.609	2.5%
	10^{-5} 10 Hz PSA	1.963	1.917	2.4%
	10^{-6} 10 Hz PSA	4.542	4.458	1.9%
	10^{-4} 1 Hz PSA	0.115	0.113	1.8%
	10^{-5} 1 Hz PSA	0.288	0.282	2.1%
	10^{-6} 1 Hz PSA	0.677	0.667	1.6%
Houston	10^{-4} PGA	0.039	0.037	3.1%
	10^{-5} PGA	0.140	0.135	3.6%
	10^{-6} PGA	0.593	0.571	3.9%
	10^{-4} 10 Hz PSA	0.081	0.079	2.8%
	10^{-5} 10 Hz PSA	0.288	0.279	3.4%
	10^{-6} 10 Hz PSA	1.078	1.044	3.3%
	10^{-4} 1 Hz PSA	0.045	0.044	2.3%
	10^{-5} 1 Hz PSA	0.124	0.120	3.2%
	10^{-6} 1 Hz PSA	0.274	0.266	3.2%
Jackson	10^{-4} PGA	0.108	0.106	2.4%
	10^{-5} PGA	0.305	0.297	2.8%
	10^{-6} PGA	1.035	1.000	3.5%
	10^{-4} 10 Hz PSA	0.226	0.221	2.5%
	10^{-5} 10 Hz PSA	0.620	0.605	2.3%
	10^{-6} 10 Hz PSA	1.804	1.757	2.7%
	10^{-4} 1 Hz PSA	0.095	0.091	4.7%
	10^{-5} 1 Hz PSA	0.221	0.213	3.9%
	10^{-6} 1 Hz PSA	0.451	0.437	3.4%
Manchester	10^{-4} PGA	0.247	0.240	2.8%
	10^{-5} PGA	0.904	0.879	2.9%
	10^{-6} PGA	2.268	2.218	2.2%
	10^{-4} 10 Hz PSA	0.463	0.452	2.6%
	10^{-5} 10 Hz PSA	1.609	1.572	2.4%
	10^{-6} 10 Hz PSA	3.991	3.914	2.0%
	10^{-4} 1 Hz PSA	0.069	0.068	1.0%
	10^{-5} 1 Hz PSA	0.217	0.214	1.6%
	10^{-6} 1 Hz PSA	0.610	0.601	1.6%
Savannah	10^{-4} PGA	0.304	0.329	-7.4%
	10^{-5} PGA	0.805	0.886	-9.2%
	10^{-6} PGA	1.890	1.996	-5.3%
	10^{-4} 10 Hz PSA	0.616	0.667	-7.6%
	10^{-5} 10 Hz PSA	1.588	1.766	-10.0%
	10^{-6} 10 Hz PSA	3.568	3.886	-8.2%
	10^{-4} 1 Hz PSA	0.151	0.163	-7.5%
	10^{-5} 1 Hz PSA	0.376	0.426	-11.8%
	10^{-6} 1 Hz PSA	0.799	0.920	-13.1%
Topeka	10^{-4} PGA	0.124	0.120	3.3%

Demonstration Site	Ground Motion Parameter	Ground Motion Level (g)		Percent Difference
		This Calculation	NUREG-2115 Chapter 8	
	10^{-5} PGA	0.512	0.493	3.7%
	10^{-6} PGA	1.621	1.562	3.8%
	10^{-4} 10 Hz PSA	0.243	0.236	3.0%
	10^{-5} 10 Hz PSA	0.921	0.891	3.4%
	10^{-6} 10 Hz PSA	2.622	2.553	2.7%
	10^{-4} 1 Hz PSA	0.069	0.068	1.8%
	10^{-5} 1 Hz PSA	0.177	0.172	2.6%
	10^{-6} 1 Hz PSA	0.397	0.388	2.3%

Table 2.5.2-233: Comparison of Reference and Deaggregation Earthquakes Based on Updated EPRI-SOG and CEUS SSC Models

Hazard	Reference (Controlling) Earthquake CEUS SSC Model		Deaggregation Earthquakes CEUS SSC Model			Reference (Controlling) Earthquake Updated EPRI-SOG Model		Deaggregation Earthquakes Updated EPRI-SOG Model		
	Magnitude (M)	Distance (km)	Magnitude (M)	Distance (km)	Weight	Magnitude (m_b)	Distance (km)	Magnitude (m_b)	Distance (km)	Weight
Mean 10^{-3} 5 and 10 Hz	6.8	372	5.3	79.7	0.102	6.6	302	5.3	63.7	0.180
			6.1	148	0.049			6.0	139	0.060
			7.0	472	0.849			6.9	464	0.760
Mean 10^{-3} 1 and 2.5Hz	6.9 7.0*	407 451*	5.4	64.4	0.053	6.8 6.9*	368 442*	5.4	49.7	0.079
			6.1	152	0.039			6.1	141	0.047
			7.0	479	0.908			6.9	469	0.874
Mean 10^{-4} 5 and 10 Hz	6.8	238	5.4	39.1	0.213	6.5	161	5.4	27.7	0.320
			6.3	90	0.076			6.2	70	0.077
			7.2	460	0.711			7.1	455	0.603
Mean 10^{-4} 1 and 2.5Hz	7.0 7.2*	326 444*	5.5	28.6	0.089	6.9 7.1*	299 447*	5.5	20.2	0.105
			6.4	86	0.054			6.3	72	0.052
			7.2	464	0.857			7.1	459	0.843
Mean 10^{-5} 5 and 10 Hz	6.2	64	5.4	19.5	0.494	6.0	34	5.4	13.6	0.615
			6.5	43	0.179			6.3	29	0.156
			7.3	456	0.328			7.2	453	0.229
Mean 10^{-5} 1 and 2.5Hz	6.9 7.3*	165 436*	5.5	16.0	0.215	6.7 7.1*	159 446*	5.6	12.2	0.218
			6.5	55	0.128			6.4	45	0.112
			7.3	459	0.657			7.2	456	0.670
Mean 10^{-6} 5 and 10 Hz	5.9	14.2	5.5	10.3	0.657	5.8	11	5.4	8.9	0.681
			6.5	20	0.323			6.4	15	0.297
			7.4	450	0.020			7.2	450	0.022
Mean 10^{-6} 1 and 2.5Hz	5.7 7.4*	42 422	5.7	10.2	0.400	6.4 7.2*	50 443*	5.7	8.9	0.400
			6.7	36	0.330			6.5	32	0.240
			7.4	457	0.270			7.2	455	0.360

*computed using earthquakes with distances > 100 km

Table 2.5.2-234

Comparison of Updated EPRI SOG Scaled GMRS with CAV and CEUS GMRS with Modified CAV

Frequency (Hz)	5% Damped Horizontal Spectral Acceleration (g)			5% Damped Vertical Spectral Acceleration (g)		
	Scaled GMRS Based on Updated EPRI-SOG Model with Full CAV	GMRS Based on CEUS SSC Model with Modified CAV	Percent Difference	Scaled GMRS Based on Updated EPRI-SOG Model with Full CAV	GMRS Based on CEUS SSC Model with Modified CAV	Percent Difference
100.0000	0.0838	0.0731	-12.8%	0.0624	0.0544	-12.8%
60.2410	0.1031	0.0905	-12.2%	0.0786	0.0690	-12.2%
50.0000	0.1170	0.1025	-12.4%	0.0934	0.0819	-12.4%
40.0000	0.1307	0.1139	-12.9%	0.1142	0.0996	-12.9%
33.3333	0.1430	0.1240	-13.3%	0.1286	0.1116	-13.3%
30.3030	0.1482	0.1286	-13.3%	0.1325	0.1149	-13.3%
25.0000	0.1726	0.1483	-14.1%	0.1500	0.1289	-14.1%
23.8095	0.1773	0.1526	-14.0%	0.1526	0.1313	-14.0%
22.7273	0.1820	0.1567	-13.9%	0.1547	0.1332	-13.9%
21.7391	0.1865	0.1608	-13.8%	0.1567	0.1351	-13.8%
20.8333	0.1910	0.1648	-13.7%	0.1579	0.1363	-13.7%
20.0000	0.1954	0.1687	-13.6%	0.1591	0.1374	-13.6%
18.1818	0.2049	0.1774	-13.4%	0.1606	0.1390	-13.4%
16.6667	0.2140	0.1857	-13.2%	0.1615	0.1401	-13.2%
15.3846	0.2227	0.1937	-13.0%	0.1630	0.1418	-13.0%
14.2857	0.2311	0.2014	-12.9%	0.1649	0.1437	-12.9%
13.3333	0.2392	0.2088	-12.7%	0.1668	0.1456	-12.7%
12.5000	0.2470	0.2160	-12.5%	0.1684	0.1473	-12.5%
11.7647	0.2515	0.2198	-12.6%	0.1680	0.1468	-12.6%
11.1111	0.2528	0.2214	-12.4%	0.1655	0.1449	-12.4%
10.5263	0.2541	0.2229	-12.3%	0.1631	0.1430	-12.3%
10.0000	0.2553	0.2243	-12.1%	0.1608	0.1412	-12.1%
9.0909	0.2578	0.2274	-11.8%	0.1596	0.1408	-11.8%
8.3333	0.2601	0.2302	-11.5%	0.1598	0.1414	-11.5%
7.6923	0.2529	0.2249	-11.0%	0.1542	0.1372	-11.0%
7.1429	0.2464	0.2201	-10.6%	0.1492	0.1333	-10.6%
6.6667	0.2405	0.2158	-10.3%	0.1447	0.1299	-10.3%
6.2500	0.2355	0.2119	-10.0%	0.1413	0.1272	-10.0%
5.8824	0.2310	0.2084	-9.8%	0.1386	0.1250	-9.8%
5.5556	0.2268	0.2051	-9.6%	0.1361	0.1231	-9.6%
5.2632	0.2229	0.2020	-9.3%	0.1337	0.1212	-9.3%
5.0000	0.2192	0.1992	-9.1%	0.1315	0.1195	-9.1%
4.5455	0.2111	0.1936	-8.3%	0.1267	0.1162	-8.3%
4.1667	0.2040	0.1887	-7.5%	0.1224	0.1132	-7.5%
3.8462	0.1977	0.1842	-6.8%	0.1186	0.1105	-6.8%
3.5714	0.1920	0.1802	-6.1%	0.1152	0.1081	-6.1%
3.3333	0.1869	0.1766	-5.5%	0.1121	0.1059	-5.5%
3.1250	0.1822	0.1732	-4.9%	0.1093	0.1039	-4.9%
2.9412	0.1779	0.1701	-4.4%	0.1067	0.1021	-4.4%
2.7778	0.1739	0.1673	-3.8%	0.1044	0.1004	-3.8%
2.6316	0.1703	0.1646	-3.3%	0.1022	0.0988	-3.3%
2.5000	0.1669	0.1621	-2.9%	0.1001	0.0973	-2.9%

Frequency (Hz)	5% Damped Horizontal Spectral Acceleration (g)			5% Damped Vertical Spectral Acceleration (g)		
	Scaled GMRS Based on Updated EPRI-SOG Model with Full CAV	GMRS Based on CEUS SSC Model with Modified CAV	Percent Difference	Scaled GMRS Based on Updated EPRI-SOG Model with Full CAV	GMRS Based on CEUS SSC Model with Modified CAV	Percent Difference
2.3810	0.1633	0.1593	-2.4%	0.0980	0.0956	-2.4%
2.2727	0.1600	0.1568	-2.0%	0.0960	0.0941	-2.0%
2.1739	0.1569	0.1543	-1.6%	0.0941	0.0926	-1.6%
2.0833	0.1540	0.1520	-1.3%	0.0924	0.0912	-1.3%
2.0000	0.1512	0.1499	-0.9%	0.0907	0.0899	-0.9%
1.8182	0.1450	0.1451	0.1%	0.0870	0.0871	0.1%
1.6667	0.1396	0.1409	0.9%	0.0837	0.0845	0.9%
1.5385	0.1337	0.1353	1.2%	0.0802	0.0812	1.2%
1.4286	0.1264	0.1286	1.7%	0.0758	0.0771	1.7%
1.3333	0.1200	0.1226	2.2%	0.0720	0.0736	2.2%
1.2500	0.1125	0.1154	2.6%	0.0675	0.0693	2.6%
1.1765	0.1059	0.1091	3.0%	0.0636	0.0654	3.0%
1.1111	0.1001	0.1034	3.3%	0.0600	0.0620	3.3%
1.0526	0.0948	0.0983	3.6%	0.0569	0.0590	3.6%
1.0000	0.0901	0.0937	3.9%	0.0541	0.0562	3.9%
0.9091	0.0845	0.0875	3.6%	0.0507	0.0525	3.6%
0.8333	0.0796	0.0823	3.3%	0.0478	0.0494	3.3%
0.7692	0.0754	0.0778	3.1%	0.0453	0.0467	3.1%
0.7143	0.0718	0.0738	2.8%	0.0431	0.0443	2.8%
0.6667	0.0685	0.0702	2.6%	0.0411	0.0421	2.6%
0.6250	0.0655	0.0671	2.4%	0.0393	0.0403	2.4%
0.5882	0.0629	0.0643	2.2%	0.0377	0.0386	2.2%
0.5556	0.0605	0.0617	2.0%	0.0363	0.0370	2.0%
0.5263	0.0583	0.0594	1.8%	0.0350	0.0356	1.8%
0.5000	0.0564	0.0573	1.6%	0.0338	0.0344	1.6%
0.4545	0.0487	0.0494	1.4%	0.0292	0.0296	1.4%
0.4167	0.0426	0.0432	1.3%	0.0256	0.0259	1.3%
0.3846	0.0377	0.0381	1.1%	0.0226	0.0229	1.1%
0.3571	0.0337	0.0340	1.0%	0.0202	0.0204	1.0%
0.3333	0.0303	0.0305	0.8%	0.0182	0.0183	0.8%
0.3125	0.0275	0.0277	0.7%	0.0165	0.0166	0.7%
0.2941	0.0252	0.0253	0.6%	0.0151	0.0152	0.6%
0.2778	0.0232	0.0233	0.5%	0.0139	0.0140	0.5%
0.2632	0.0214	0.0215	0.4%	0.0129	0.0129	0.4%
0.2500	0.0199	0.0200	0.3%	0.0119	0.0120	0.3%
0.2381	0.0186	0.0186	0.2%	0.0112	0.0112	0.2%
0.2273	0.0174	0.0174	0.1%	0.0104	0.0105	0.1%
0.2174	0.0163	0.0163	0.0%	0.0098	0.0098	0.0%
0.2083	0.0154	0.0154	-0.1%	0.0092	0.0092	-0.1%
0.2000	0.0145	0.0145	-0.1%	0.0087	0.0087	-0.1%
0.1818	0.0127	0.0126	-0.3%	0.0076	0.0076	-0.3%
0.1667	0.0112	0.0112	-0.5%	0.0067	0.0067	-0.5%
0.1538	0.0100	0.0099	-0.6%	0.0060	0.0060	-0.6%
0.1429	0.0090	0.0089	-0.8%	0.0054	0.0054	-0.8%
0.1333	0.0081	0.0081	-0.9%	0.0049	0.0048	-0.9%
0.1250	0.0074	0.0073	-1.0%	0.0044	0.0044	-1.0%
0.1176	0.0068	0.0067	-1.1%	0.0041	0.0040	-1.1%
0.1111	0.0062	0.0061	-1.2%	0.0037	0.0037	-1.2%
0.1000	0.0053	0.0052	-1.4%	0.0032	0.0031	-1.4%

Table 2.5.2-235

Comparison of Updated EPRI SOG Scaled PBSRS with CAV and CEUS PBSRS with Modified CAV

Frequency (Hz)	5% Damped Horizontal Spectral Acceleration (g)			5% Damped Vertical Spectral Acceleration (g)		
	Scaled PBSRS Based on Updated EPRI-SOG Model with Full CAV	PBSRS Based on CEUS SSC Model with Modified CAV	Percent Difference	Scaled PBSRS Based on Updated EPRI-SOG Model with Full CAV	PBSRS Based on CEUS SSC Model with Modified CAV	Percent Difference
100.0000	0.1293	0.1014	-21.6%	0.0899	0.0705	-21.6%
60.2410	0.1535	0.1231	-19.8%	0.1094	0.0877	-19.8%
50.0000	0.1704	0.1378	-19.2%	0.1350	0.1091	-19.2%
40.0000	0.1829	0.1485	-18.8%	0.1607	0.1305	-18.8%
33.3333	0.1973	0.1594	-19.2%	0.1847	0.1493	-19.2%
30.3030	0.2030	0.1638	-19.3%	0.1915	0.1546	-19.3%
25.0000	0.2348	0.1878	-20.0%	0.2114	0.1691	-20.0%
23.8095	0.2427	0.1943	-19.9%	0.2155	0.1726	-19.9%
22.7273	0.2504	0.2007	-19.8%	0.2178	0.1746	-19.8%
21.7391	0.2580	0.2071	-19.7%	0.2200	0.1765	-19.7%
20.8333	0.2656	0.2134	-19.6%	0.2221	0.1784	-19.6%
20.0000	0.2730	0.2196	-19.6%	0.2241	0.1803	-19.6%
18.1818	0.2863	0.2307	-19.4%	0.2244	0.1808	-19.4%
16.6667	0.3025	0.2435	-19.5%	0.2251	0.1813	-19.5%
15.3846	0.3220	0.2585	-19.7%	0.2296	0.1843	-19.7%
14.2857	0.3308	0.2664	-19.5%	0.2286	0.1841	-19.5%
13.3333	0.3391	0.2739	-19.2%	0.2279	0.1841	-19.2%
12.5000	0.3452	0.2800	-18.9%	0.2267	0.1839	-18.9%
11.7647	0.3510	0.2852	-18.7%	0.2255	0.1833	-18.7%
11.1111	0.3566	0.2902	-18.6%	0.2247	0.1829	-18.6%
10.5263	0.3620	0.2951	-18.5%	0.2255	0.1838	-18.5%
10.0000	0.3644	0.2979	-18.3%	0.2246	0.1836	-18.3%
9.0909	0.3696	0.3039	-17.8%	0.2228	0.1832	-17.8%
8.3333	0.3745	0.3095	-17.3%	0.2209	0.1826	-17.3%
7.6923	0.3792	0.3147	-17.0%	0.2203	0.1828	-17.0%
7.1429	0.3836	0.3195	-16.7%	0.2217	0.1847	-16.7%
6.6667	0.3828	0.3200	-16.4%	0.2202	0.1841	-16.4%
6.2500	0.3811	0.3195	-16.1%	0.2182	0.1830	-16.1%
5.8824	0.3777	0.3176	-15.9%	0.2154	0.1812	-15.9%
5.5556	0.3746	0.3153	-15.8%	0.2128	0.1791	-15.8%
5.2632	0.3669	0.3084	-15.9%	0.2077	0.1746	-15.9%
5.0000	0.3597	0.3029	-15.8%	0.2036	0.1715	-15.8%
4.5455	0.3272	0.2772	-15.3%	0.1852	0.1569	-15.3%
4.1667	0.2982	0.2541	-14.8%	0.1688	0.1438	-14.8%
3.8462	0.2746	0.2353	-14.3%	0.1554	0.1332	-14.3%
3.5714	0.2552	0.2197	-13.9%	0.1445	0.1244	-13.9%
3.3333	0.2390	0.2070	-13.4%	0.1357	0.1175	-13.4%
3.1250	0.2256	0.1962	-13.0%	0.1285	0.1118	-13.0%
2.9412	0.2132	0.1862	-12.7%	0.1219	0.1065	-12.7%
2.7778	0.2084	0.1825	-12.4%	0.1195	0.1047	-12.4%
2.6316	0.2040	0.1790	-12.2%	0.1173	0.1030	-12.2%
2.5000	0.1998	0.1758	-12.0%	0.1154	0.1015	-12.0%
2.3810	0.1959	0.1726	-11.9%	0.1136	0.1001	-11.9%
2.2727	0.1922	0.1697	-11.7%	0.1119	0.0988	-11.7%
2.1739	0.1888	0.1669	-11.6%	0.1104	0.0975	-11.6%
2.0833	0.1856	0.1642	-11.5%	0.1089	0.0964	-11.5%

Frequency (Hz)	5% Damped Horizontal Spectral Acceleration (g)			5% Damped Vertical Spectral Acceleration (g)		
	Scaled PBSRS Based on Updated EPRI-SOG Model with Full CAV	PBSRS Based on CEUS SSC Model with Modified CAV	Percent Difference	Scaled PBSRS Based on Updated EPRI-SOG Model with Full CAV	PBSRS Based on CEUS SSC Model with Modified CAV	Percent Difference
2.0000	0.1825	0.1618	-11.4%	0.1076	0.0953	-11.4%
1.8182	0.1756	0.1565	-10.9%	0.1045	0.0931	-10.9%
1.6667	0.1695	0.1519	-10.4%	0.1013	0.0908	-10.4%
1.5385	0.1628	0.1464	-10.1%	0.0981	0.0881	-10.1%
1.4286	0.1548	0.1399	-9.6%	0.0941	0.0851	-9.6%
1.3333	0.1477	0.1334	-9.7%	0.0904	0.0817	-9.7%
1.2500	0.1381	0.1250	-9.5%	0.0850	0.0770	-9.5%
1.1765	0.1296	0.1176	-9.3%	0.0802	0.0728	-9.3%
1.1111	0.1221	0.1110	-9.1%	0.0760	0.0690	-9.1%
1.0526	0.1154	0.1051	-9.0%	0.0722	0.0657	-9.0%
1.0000	0.1094	0.0998	-8.8%	0.0687	0.0627	-8.8%
0.9091	0.1019	0.0926	-9.1%	0.0641	0.0583	-9.1%
0.8333	0.0955	0.0865	-9.4%	0.0602	0.0546	-9.4%
0.7692	0.0899	0.0813	-9.6%	0.0568	0.0513	-9.6%
0.7143	0.0851	0.0767	-9.8%	0.0538	0.0485	-9.8%
0.6667	0.0808	0.0727	-10.0%	0.0512	0.0460	-10.0%
0.6250	0.0770	0.0691	-10.2%	0.0488	0.0438	-10.2%
0.5882	0.0736	0.0659	-10.4%	0.0467	0.0419	-10.4%
0.5556	0.0705	0.0631	-10.6%	0.0448	0.0401	-10.6%
0.5263	0.0677	0.0604	-10.8%	0.0431	0.0385	-10.8%
0.5000	0.0652	0.0581	-10.9%	0.0415	0.0370	-10.9%
0.4545	0.0562	0.0499	-11.1%	0.0358	0.0318	-11.1%
0.4167	0.0490	0.0435	-11.2%	0.0312	0.0277	-11.2%
0.3846	0.0432	0.0383	-11.3%	0.0275	0.0244	-11.3%
0.3571	0.0385	0.0341	-11.4%	0.0245	0.0217	-11.4%
0.3333	0.0346	0.0306	-11.5%	0.0220	0.0195	-11.5%
0.3125	0.0313	0.0277	-11.6%	0.0200	0.0176	-11.6%
0.2941	0.0286	0.0252	-11.7%	0.0182	0.0161	-11.7%
0.2778	0.0263	0.0232	-11.8%	0.0167	0.0148	-11.8%
0.2632	0.0243	0.0214	-11.9%	0.0155	0.0136	-11.9%
0.2500	0.0225	0.0198	-12.0%	0.0144	0.0126	-12.0%
0.2381	0.0210	0.0185	-12.0%	0.0134	0.0118	-12.0%
0.2273	0.0197	0.0173	-12.1%	0.0125	0.0110	-12.1%
0.2174	0.0184	0.0162	-12.2%	0.0117	0.0103	-12.2%
0.2083	0.0173	0.0152	-12.3%	0.0110	0.0097	-12.3%
0.2000	0.0164	0.0143	-12.3%	0.0104	0.0091	-12.3%
0.1818	0.0143	0.0125	-12.5%	0.0091	0.0079	-12.5%
0.1667	0.0126	0.0110	-12.6%	0.0080	0.0070	-12.6%
0.1538	0.0112	0.0098	-12.7%	0.0071	0.0062	-12.7%
0.1429	0.0100	0.0088	-12.8%	0.0064	0.0056	-12.8%
0.1333	0.0091	0.0079	-13.0%	0.0058	0.0050	-13.0%
0.1250	0.0082	0.0072	-13.1%	0.0053	0.0046	-13.1%
0.1176	0.0075	0.0065	-13.1%	0.0048	0.0042	-13.1%
0.1111	0.0069	0.0060	-13.2%	0.0044	0.0038	-13.2%
0.1000	0.0059	0.0051	-13.4%	0.0037	0.0032	-13.4%

Revised FSAR Figures

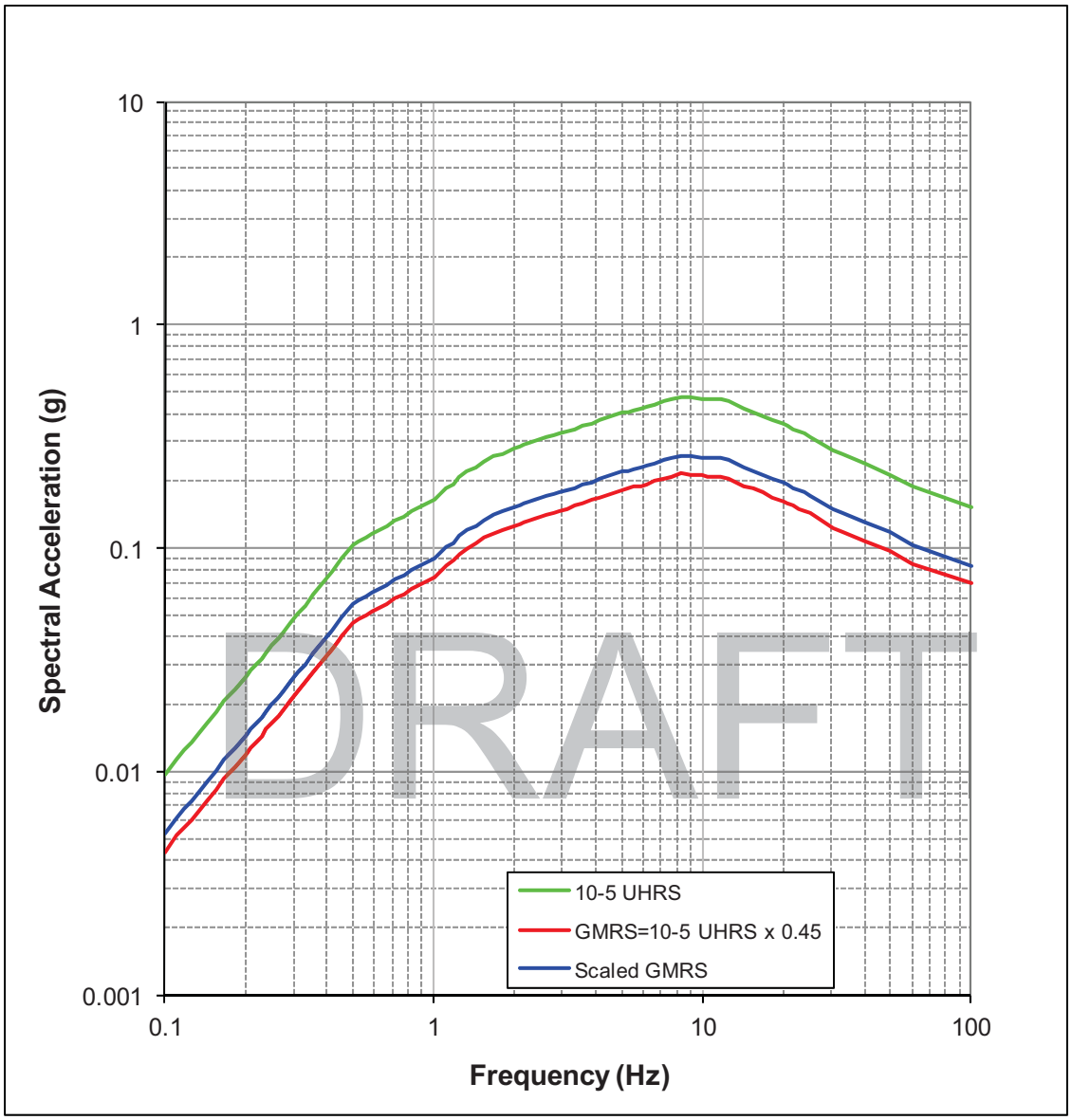

Revised Figure 2.5.2-294: Horizontal 10^{-5} UHRS, GMRS, and Scaled GMRS Based on CAV for the LNP Site.

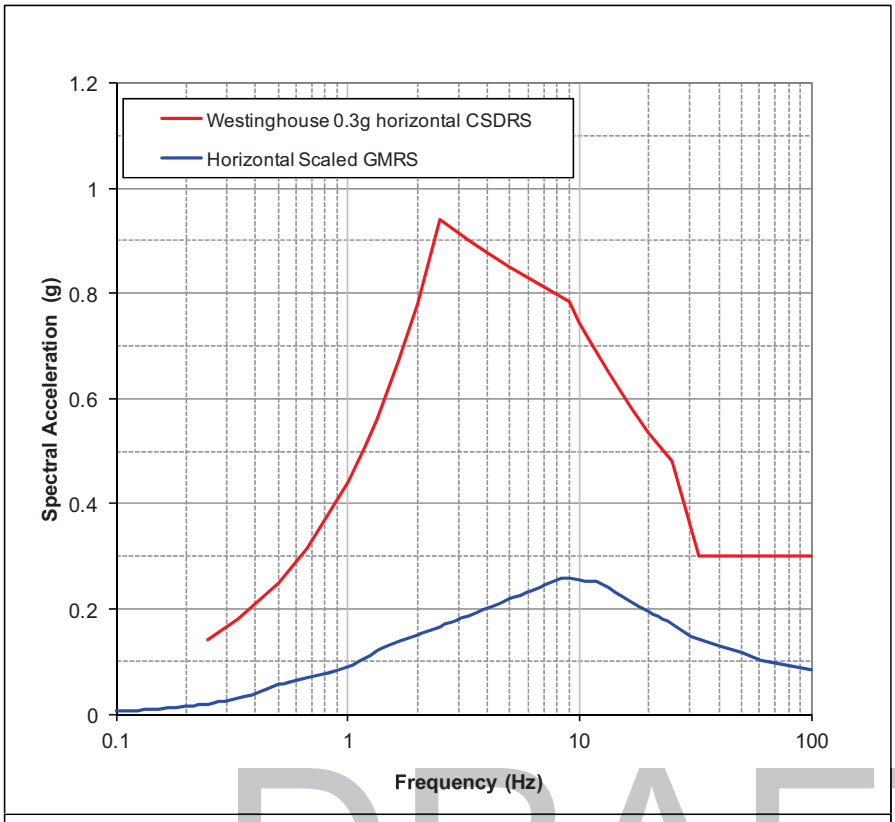

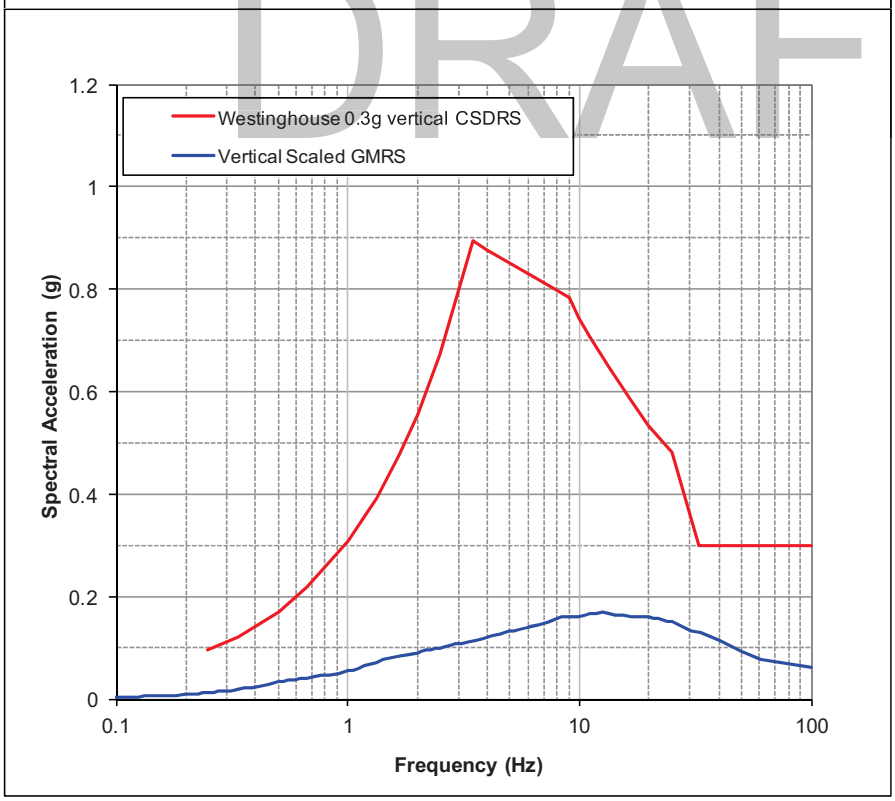

Revised Figure 2.5.2-296: Horizontal and Vertical Scaled GMRS for the LNP Site.